

Can new particle formation occur in the clean marine boundary layer?

Liisa Pirjola and Colin D. O'Dowd^{1,2}

Department of Physics, University of Helsinki, Helsinki, Finland

Ian M. Brooks

Scripps Institution of Oceanography, La Jolla, California

Markku Kulmala

Department of Physics, University of Helsinki, Helsinki, Finland

Abstract. An analysis of new particle formation probability in the marine boundary layer (MBL) is conducted using a detailed aerosol dynamics and gas-phase chemistry model, thermodynamically correct classical binary ($\text{H}_2\text{O}-\text{H}_2\text{SO}_4$) nucleation theory, and recently developed ternary ($\text{H}_2\text{O}-\text{H}_2\text{SO}_4-\text{NH}_3$) nucleation theory. Additionally, the effect of boundary-layer meteorology (i.e., adiabatic cooling, small scale fluctuations, and entrainment) in enhancing nucleation is also examined. The results indicate that for typical marine conditions, binary nucleation does not occur for any realistic conditions regardless of adiabatic cooling, turbulent fluctuations, or entrainment. For polar marine conditions, binary nucleation does occur due to lower temperatures, and is enhanced due to turbulent fluctuations. An increase in detectable particle sizes ($N_3 > 3$ nm), is only seen after multiple boundary layer circulations for conditions of high dimethyl sulphide (DMS) concentrations (400 ppt). Under extreme conditions of entrainment of free-troposphere layers containing very low aerosol condensation sinks and extraordinary high sulphuric acid concentrations ($> 10^8$ molecules cm^{-3}), increases in detectable particles up to 10,000 cm^{-3} are predicted only in polar marine air, but are viewed as unlikely to occur in reality. Comparison of model simulations with observed values of DMS and sulphuric acid in polar marine air masses suggest that binary nucleation may lead to an enhancement of ≈ 1000 cm^{-3} in N_3 particle concentration, but not to enhancements of $\approx 10,000$ cm^{-3} . Ternary nucleation is predicted to occur under realistic sulphuric acid (1.2×10^7 molecules cm^{-3}) and ammonia (> 5 ppt) concentrations; however, significant growth to detectable sizes (N_3) only occurs for DMS concentrations of the order of 400 ppt and very low aerosol condensation sinks, but these conditions are thought to be very infrequent in the MBL and are unlikely to make a significant contribution to the general MBL aerosol concentration. It is plausible that the background MBL aerosol concentration could be maintained by a slow, almost undetectable production rate, and not by noticeable nucleation events where large enhancements in N_3 concentrations are observed. The former requires sustained DMS concentrations of the order of 100 ppt which seems unlikely. In summary, the occurrence of new particles in the unperturbed MBL would be difficult to explain by DMS emissions alone. DMS emissions can explain the occurrence of thermodynamically stable sulphate clusters, but under most conditions, to grow these clusters to detectable sizes before they are scavenged by coagulation, an additional condensable species other than DMS-derived sulphuric acid would be required. In the event, however, of significant removal of the preexisting aerosol due to precipitation, the MBL aerosol can be replenished through growth of new particle formed through ternary nucleation under moderately high DMS concentrations.

¹Also at Physics Department, National University of Ireland, Galway, University Road, Galway (corresponding address).

²Also Centre for Marine & Atmospheric Sciences, University of Sunderland, Sunderland, SR2 7BW.

Copyright 2000 by the American Geophysical Union.

Paper number 2000JD900310.
0148-0227/00/2000JD900310\$09.00

1. Introduction

Marine stratiform clouds contribute significantly to the global planetary radiation budget due to their extensive coverage and the low underlying ocean-surface albedo [Houghton *et al.*, 1995]. Not only do these clouds contribute to the global albedo, they are thought to comprise one of the most sensitive cloud-radiation systems due to their high susceptibility to change resulting from their generally low droplet concentration [Slingo, 1990]. As a result of their global importance and high susceptibility,

considerable effort has been dedicated to understanding physical and chemical mechanisms that control their microphysical properties [Baker and Charlson, 1990; Durkee et al., 2000; O'Dowd et al., 1999a, 1999b]. The two most important factors determining cloud properties are vertical updraft and cloud condensation nuclei (CCN) availability [Pruppacher and Klett, 1978]. In terms of CCN, there are two primary sources in the unperturbed marine boundary layer (MBL) [Dinger et al., 1970]: mechanically produced sea-salt nuclei and non-sea-salt (nss) sulphate produced through gas-to-particle conversion processes. The dominant source of nss-sea-salt is through the production of sulphuric acid, methane sulphonic acid (MSA) and SO₂ via dimethyl sulphide (DMS) oxidation [Yin et al., 1990]. Both sulphuric acid and MSA can condense onto existing particles and provide additional aerosol mass, thus increasing the CCN efficiency of preexisting aerosols, while SO₂ can be absorbed into existing aerosol and cloud droplets [Sievering et al., 1992; Hoppel et al., 1994] where it can be rapidly oxidised by ozone or hydrogen peroxide to produce further nss-sulphate mass. The preexisting nss-sulphate aerosol in the marine boundary layer can either be produced locally within the boundary layer or by entrainment from the free troposphere [Raes, 1995]; however, it is not clearly known which of these sources prevail, and thus control the remote marine boundary layer nss-sulphate aerosol concentration. Additionally, anthropogenic and/or continental contributions can be significant to the marine boundary layer aerosol, even thousands of kilometers out over the ocean, particularly in the Northern Hemisphere [O'Dowd et al., 1993; Osborne et al., 2000].

The dominant source of these particles has been the subject of extensive investigation and debate over the last decade or so. Many modeling studies, ranging from single mode models [Kreidenweis and Seinfeld, 1988; Baker and Charlson, 1990], integral bimodal models [Hegg, 1990], high size resolution sectional models [Raes and Van Dingenen, 1992; Lin et al., 1992] to dynamic and steady-state two-size section models [Pandis et al., 1994; Russell et al., 1994] have tried to relate CCN production to DMS emissions and oxidation. The wide variety of approaches has led to discrepancies in predicted results and to conflicting opinions in the literature [Raes and Van Dingenen, 1995; Pandis et al., 1995] which still have not resolved the issue of particle production in the MBL. While some of these discrepancies seem to relate to the degree of detail in representing the aerosol size distributions and effects this will have on simulation results, one of the primary sources of error in all of the above studies relates to determining, within a reasonable degree of accuracy, the nucleation rate of new particles for MBL conditions. Models treating only binary nucleation required the use of a nucleation rate tuner ranging from 10⁴ to 10⁵ due to the apparent inability of classical nucleation theory to predict nucleation rates accurately. In all of these previous studies, only binary nucleation has been considered.

To date, the most comprehensive studies of processes governing the aerosol MBL population is that by Katoshevski et al. [1999] and Capaldo et al. [1999]. Capaldo et al. [1999] considered spatial and temporal variability of parameters relevant to new particle formation, while Katoshevski et al. [1999] attempted to account for ternary nucleation by increasing the nucleation rate tuner to 10¹⁰ and 10¹⁶ and concluded that, while entrainment from the free troposphere tended to sustain particle concentrations, enhanced nucleation rates in the MBL were able to significantly enhance, and provide a controlling influence on, the long-term MBL aerosol concentrations. While this model study extensively addressed most of the boundary layer aerosol processes, the question of what actually controls the source and concentration of marine aerosols remains unanswered until the

probability of binary and ternary nucleation is more accurately quantified and represented in models rather than simply using nucleation tuners.

To address the importance of in situ particle production in the MBL, one must also examine the experimental evidence that may support the concept of the MBL as being a source of particle production. As pointed out by Katoshevski et al. [1999], it appears from experimental measurements that nucleation is quite a rare occurrence in the MBL. In fact, new particle formation, or nucleation, is never strictly observed since current aerosol measurement technology does not allow measurement of actual new particles thought to possess a critical size of around 1 nm. Typically, the current lower measurement detection limit is 3 nm, and consequently, only recently formed particles that have grown to 3 nm sizes through coagulation and/or condensation are detected. The lack of 3 nm particle occurrence does not, however, mean that nucleation is not occurring, it can also mean that nucleation is occurring but the new particles are scavenged by coagulation with preexisting particles over timescales shorter than that required for growth by self-coagulation and/or condensation. Recent studies on ternary nucleation suggest that thermodynamically stable sulphate clusters (TSCs) can form readily and rapidly through ternary sulphuric acid-ammonia-water nucleation and that these TSCs only produce detectable particles if condensational growth is sufficiently rapid compared to their loss rate [Kulmala et al., 2000]. In other words, ternary nucleation can occur regularly, but these stable embryos are rapidly lost through diffusive coagulation unless there is a sufficiently strong source of condensable material available.

Over the open oceans there have been only a few recorded observations of new particle formation [Covert et al., 1992, 1996; Clarke et al., 1998; Hoppel et al., 1989]. Examination of experimental data indicates that under typical marine conditions, nucleation does not occur. Ultrafine particles observed over the Pacific by Covert et al. [1992] could be explained by entrainment from the free troposphere, while ultrafine particle concentration observed in the tropics were considered to result from in situ particle nucleation relating to the natural DMS cycle [Clarke et al., 1998]. Frequent occurrence of ultrafine particles also occurs in polar marine air masses and have been observed quite regularly during one particular Antarctic cruise [O'Dowd et al., 1997a]. Almost all cases of ultrafine particle occurrence were associated with a reduction in preexisting aerosol surface area, and consequently, condensation sink potential. In contrast to observations of ultrafine particle occurrence after reductions in aerosol surface area, a number of studies have supported the concept of particle nucleation in cloud, despite the exceptionally high condensation sink available [Hegg et al., 1990].

In comparison to the open ocean, very high ultrafine particle concentrations, with a high frequency of occurrence, is observed in the coastal environment [O'Dowd et al., 1998]. In a detailed study to attempt to determine the processes leading to this occurrence, O'Dowd et al. [1999c] found that ternary nucleation was likely to be occurring more times than ultrafine particles were observed, and that the presence of these ultrafine particles could only be explained if an additional source of condensable species, other than sulphuric acid, was available to grow new particles to detectable sizes.

While there have been observations of ultrafine particles, it is not clear whether or not these occurred through binary or ternary nucleation processes or whether sulphuric acid could also account for growth of new particles into quasi-static condensation nuclei sizes. In this study, we simulate boundary layer nucleation processes using realistic aerosol and gas phase concentrations. In addition, we apply realistic BL meteorological scenarios which are capable of promoting and enhancing nucleation in an attempt

to determine whether or not new, and ultrafine particle formation can occur in the marine boundary layer or whether another source of particles is required.

2. Boundary Layer Meteorological Processes and Nucleation

The binary nucleation rate is strongly dependent on temperature T , relative humidity (RH), and the partial pressure of H_2SO_4 [Kulmala, 1990]. The equilibrium vapor pressure of H_2SO_4 is also dependent on relative humidity. The highly nonlinear nature of these dependencies means that small changes in temperature and relative humidity can result in large changes of the nucleation rate. There are a number of dynamic processes within the marine boundary layer that can lead to changes in T and RH sufficient to significantly affect the nucleation rate. It is thus insufficient to consider mean boundary layer conditions alone when determining nucleation rates; the effects of small-scale variability must also be accounted for.

The boundary layer processes affecting nucleation rates can be conveniently divided into three groups [Nilsson and Kulmala, 1998]. First, large scale processes in which air parcels are subject to vertical motions on the scale of the order of the boundary layer depth leading to adiabatic heating or cooling of the entire parcel. Such processes include the largest scale eddies within the turbulent BL, convective plumes, roll circulations, and gravity waves. The second class is small-scale turbulence that generates small changes in T and RH about the local means. Easter and Peters [1994] modeled the effects of turbulence on nucleation within a marine boundary layer and found that the nucleation rate could be enhanced by up to 70 times if the fluctuations in T and RH were anticorrelated. It should, however, be noted that a distinct air parcel does not undergo changes in T and RH in isolation from its surroundings, but that the fluctuations result from the small scale mixing of neighboring air parcels with slightly different properties. If we assume that the differences in T and humidity between two parcels are independent, then the resulting mixture may be warmer and moister, warmer and drier, cooler and moister, or cooler and drier than our original parcel. For simplicity in the model, we can consider only the initial and final states and apply random fluctuations of T and RH to a single air parcel as if they occurred in isolation. The relative distribution of positive and negative fluctuations of T and RH is dependent on the structure of the boundary layer and the location within it. In stable conditions, air originating below a given level will tend to be cooler and moister, while air from above will be warmer and drier. In a highly convective boundary layer such as occurs where cold air is advected over warmer water the distribution will be skewed to warmer and moister air from below, and cooler, drier air from above. In a near-neutral or weakly convective boundary layer the distribution will be more uniform. We consider such a near neutral case and assume that the fluctuations, due to turbulent mixing, in T and RH are independent.

The final class of processes to be considered is mixing between two air parcels with large differences in their initial values of T and RH. Mixing of different air masses may lead to a substantial increase in nucleation rate; the modeling study of Nilsson and Kulmala, [1998] suggested an increase of up to three orders of magnitude. Within a marine boundary layer the largest gradients in T and RH are found across the inversion, substantial gradients may also exist across the full depth of a stable boundary layer. Significant horizontal gradients may occur over sea surface temperature fronts, at the boundaries of convective clouds, and in coastal areas across sea breeze fronts; however, only entrainment across the inversion is considered in the present study.

3. Model

3.1. Model Description

The model used in this study is a Lagrangian based sectional box model AEROFOR [Pirjola, 1999] which includes gas-phase chemistry and aerosol dynamics. The following processes are considered: (1) surface flux DMS; (2) gas-phase oxidation of DMS to SO_2/SO_3 ; (3) gas-phase oxidation of SO_2/SO_3 to H_2SO_4 ; (4) homogeneous nucleation of H_2SO_4 and H_2O ; (5) condensation of MSA, H_2SO_4 and H_2O onto preexisting particles; (6) direct reaction of SO_2 with particles; (7) Brownian coagulation of particles; (8) dry deposition to the sea surface; and (9) entrainment of air from the free troposphere. The chemical mechanism (67 species altogether) is presented by Pirjola and Kulmala [1998]; the inorganic and organic chemistry are based on the EMEP mechanism [Simpson, 1992] and the DMS chemistry is adopted from Saltelli and Hjort [1995]. In addition, the oxidation of DMS by NO_3 at nighttime has been added with the reaction rate constant $1.9 \times 10^{-13} \exp(520/T)$ [Atkinson et al., 1996].

Nucleation rate is determined using the revised, thermodynamically correct classical nucleation theory [Wilemski, 1984] taking into account the hydrate formation [Jaecker-Voirol et al., 1987]. This form of the theory predicts homogeneous nucleation in the sulphuric acid-water system rather well at least at around 298 K and at relative humidities of 30-50% [Viisanen et al., 1997]. To save computer time, we have used a parameterized value for the sulphuric acid mole fraction of the critical nucleus as a function of temperature, relative humidity and relative acidity as described by Kulmala et al. [1998]. Surface tension is adopted from Sabinina and Terpurow [1935]. Activity coefficients for water and sulphuric acid are adopted from Taleb et al. [1996].

Several field measurements, however, indicate that observed ambient nucleation rates can substantially exceed those predicted based on binary $\text{H}_2\text{SO}_4\text{-H}_2\text{O}$ [O'Dowd et al., 1998, 1999a; Clarke et al., 1998]. Recently developed classical theory of ternary $\text{H}_2\text{SO}_4\text{-NH}_3\text{-H}_2\text{O}$ nucleation [Korhonen et al., 1999] shows that if NH_3 concentration is over 100 ppt, at a H_2SO_4 concentration of 10^6 molecules cm^{-3} , significant nucleation can occur. On the other hand, when H_2SO_4 concentration exceeds 10^7 molecules cm^{-3} , around 20 ppt NH_3 is needed for significant nucleation. A preliminary parameterisation for ternary nucleation rate is included in this version of AEROFOR.

The condensation flux of H_2SO_4 onto the droplet is proportional to the difference between the vapor pressure of H_2SO_4 distant from the droplet (p_v) and at the droplet (p_{va}). The value of p_{va} is determined from the Kelvin equation, but in practice it is much less than p_v . The saturation vapor pressures for water and sulphuric acid are calculated according to Preining et al. [1981] and Ayers et al. [1980], respectively. Condensation rates are calculated using the continuum regime theory corrected by a transitional correction factor according to Fuchs and Sutugin [1970] (see details given by Kulmala, [1990] and Pirjola and Kulmala [1998]). The binary diffusion coefficient for air and condensing vapor is taken from Reid et al. [1987]. It is assumed that the particles are immediately in equilibrium with the ambient water vapor. In addition, the maximum flux of MSA onto droplets is assumed.

In the absence of clouds, gaseous SO_2 is known to react effectively with sea-salt particles [Sievering et al., 1995]. SO_2 can also react with submicron particles and promote aerosol-phase SO_2 -to-sulphate conversion. The rate coefficient R ($\text{m}^3 \text{s}^{-1}$) for the reaction of SO_2 with a single particle can be calculated by $R =$

$0.25cA\gamma$, where c (m s^{-1}) is the mean molecular speed of SO_2 in the gas phase, A is the particle surface area, and γ is the reactive uptake coefficient [Ravishankara, 1997]. Because the reactive uptake coefficient γ depends on the particle size, different values of γ are used for different modes. Kerminen *et al.* [2000] have shown that under daylight conditions condensation of sulphuric acid produced from SO_2 in the gas phase and direct reaction of SO_2 with the particulate phase become comparable to each other when γ is of the order 0.001. This value even assists the growth of very small particles to sizes necessary for CCN activation. On the other hand, estimations of γ for certain well-known reactions occurring in the aqueous phase do not seem to be high enough to account for growth into CCN size. Thus a lower value is used: 10^{-4} for particles $<1 \mu\text{m}$ in radius and 10^{-3} for particles $>1 \mu\text{m}$. Oxidation of SO_2 on particle surfaces is not considered in this work.

To conserve the mass between the gas and aerosol phase, the flux rates of H_2SO_4 , SO_2 and MSA are also taken into account in calculating the gas-phase H_2SO_4 , SO_2 , and MSA concentrations. The Brownian coagulation coefficient between particles is calculated according to Fuchs [1964], and the diffusion coefficient of a particle with the Cunningham correction factor according to Allen and Raabe [1985]. The dry deposition of particles in each section is controlled by Brownian diffusion, interception and gravitational settling [Schack *et al.*, 1985].

For the sectional representation, we have used 27 sections between the particle dry radius range 0.5 nm and 10 μm . Each section is considered as monodisperse with diameter d . All those droplets which belong to a certain section have a fixed number of H_2SO_4 molecules. The time evolution of the particle number concentration in each section is given by Raes and Janssens [1986]. The set of stiff differential equations was solved using NAG-library FORTRAN-routine D02EJF [Fortran, 1990].

3.2. Model Input Conditions

Two different air masses, maritime and polar maritime, with distinct aerosol properties are investigated. Initial meteorological parameters (at 10 m above sea level) in the maritime case are $T=10^\circ\text{C}$, $\text{RH}=70\%$, and initial total number concentration about 500 cm^{-3} while in the polar case they are -3°C , 70% , and 400 cm^{-3} , respectively. In both cases preexisting aerosol size distribution possessed Aitken and accumulation modes as well as film drop and jet drop sea-salt modes.

Typical maritime log-normal parameters for the Aitken mode are $N_{\text{Ait}} = 400 \text{ cm}^{-3}$, $r_{\text{Ait}} = 25 \text{ nm}$, $\sigma = 1.4$ and for the accumulation mode $N_{\text{acc}} = 100 \text{ cm}^{-3}$, $d_{\text{acc}} = 150 \text{ nm}$, $\sigma = 1.45$ [O'Dowd *et al.*, 1997b]. For the polar air the background CN concentration is typically $< 500 \text{ cm}^{-3}$ with the accumulation mode aerosol concentration ranging from 10-60 cm^{-3} [O'Dowd *et al.*, 1997a]. In agreement with these observations we have used $N_{\text{Ait}} = 385 \text{ cm}^{-3}$, $d_{\text{Ait}} = 40 \text{ nm}$, $\sigma = 1.4$ and $N_{\text{acc}} = 10 \text{ cm}^{-3}$, $d_{\text{acc}} = 140 \text{ nm}$, $\sigma = 1.45$, respectively.

Sea-salt particles are produced at the sea surface by the bursting of air bubbles as a result of wind stress. Sea-salt aerosol number concentration is strongly dependent on wind speed, and very often dominates the condensation sink [O'Dowd *et al.*, 1997b]; thus, simulations are run for conditions typical of low and high wind speeds, 4 m s^{-1} and 16 m s^{-1} for marine air masses and 2 m s^{-1} and 10 m s^{-1} for polar air masses, respectively. Although there is not necessarily any inherent difference between wind speeds in polar maritime or maritime air masses, a lower wind speed is taken for polar cases to account for possibly reduced sea-salt flux resulting from reduced fetch over pack-ice regions. The film drop mode possesses parameters $d_{\text{film}}=200 \text{ nm}$ and $\sigma_{\text{film}} = 1.9$, the jet drop mode $d_{\text{jet}} = 2 \mu\text{m}$ and $\sigma_{\text{jet}} = 2.0$, and

the total number concentrations for the modes are $\log N_{\text{film}} = 0.095U_{10} + 0.283$ and $\log N_{\text{jet}} = 0.0422U_{10} - 0.288$, where U_{10} is the 10 m height wind speed [O'Dowd *et al.*, 1997b].

Measurements show that DMS concentrations in air vary greatly and they have latitudinal, seasonal and diurnal trends [Andreae *et al.*, 1994; Andreae *et al.*, 1995; Bates *et al.*, 1987; Davison *et al.*, 1996; O'Dowd *et al.*, 1997a]. During one particular cruise between the England and the Antarctica in 1992-1993, on which regular new particle formation was observed in the Antarctic region, it was observed that in equatorial regions the atmospheric DMS concentration ranged from 3 to 46 ng(S)m^{-3} and in the polar waters and regions concentrations from 3 to 714 ng(S)m^{-3} were obtained [Davison *et al.*, 1996]. The peak values were associated with measurements over the broken pack ice regions, which have strong biological productivity. In this work, model calculations have been carried out with two different DMS concentrations based on these observations. Emission fluxes of gaseous DMS from the sea surface are given as 5×10^9 and 2×10^{10} molecules $\text{cm}^{-2} \text{ s}^{-1}$ causing daily peak DMS concentrations about 100 to 400 ppt which are consistent with observations in melting pack ice near Antarctica [O'Dowd *et al.*, 1997a].

The DMS oxidation by OH leads, on one hand, to the formation of SO_2 or directly to SO_3 [Bandy *et al.*, 1992; Lin and Chameides, 1993] and thus the formation of H_2SO_4 , and, on the other hand, to the formation of methane sulphonic acid ($\text{CH}_3\text{SO}_3\text{H}$, MSA). In this work DMS is the only source for SO_2 . Figure 1 illustrates the time evolution of DMS, SO_2 , H_2SO_4 and MSA in both cases: with high (1), and low (2) DMS fluxes. (It should be noted that while we refer to DMS concentrations of 100 ppt and 400 ppt as low and high, respectively, both are in fact high DMS concentrations. In this study, the reference to low and high is made to distinguish between the two regimes.) The diurnal cycle of OH (maximum value about $3.7 \times 10^6 \text{ cm}^{-3}$) is determined by the chemistry mechanism with the following initial values: $\text{O}_3 = 30 \text{ ppb}$, $\text{NO} = 0.2 \text{ ppb}$, $\text{NO}_2 = 0.8 \text{ ppb}$, $\text{HCHO} = 1 \text{ ppb}$, $\text{CH}_3\text{CHO} = 300 \text{ ppt}$, $\text{C}_2\text{H}_6 = 1 \text{ ppb}$, $\text{C}_4\text{H}_{10} = 500 \text{ ppt}$, $\text{C}_2\text{H}_4 = 300 \text{ ppt}$, $\text{C}_3\text{H}_6 = 100 \text{ ppt}$ and *o*-xylene = 100 ppt.

The primary differences between both air masses relates to lower temperature, low accumulation mode concentration, and lower sea-salt fluxes, thus leading to a lower condensation sink in the polar airmass. The maritime as well as the polar marine airmass were each classified to four types: MI – MIV and PI – PIV, respectively, corresponding conditions for low winds and low DMS flux to high wind speeds and high DMS flux. The full range of initial conditions for marine and polar simulations are summarised in Table 1. The most important parameter in terms of limiting nucleation is the preexisting aerosol condensation sink which suppresses the peak supersaturation of the nucleating vapor. The normalized condensation sink for each mode (i.e., for $N = 1 \text{ cm}^{-3}$) is given in Table 2a for dry sizes and also for wet ($\text{RH}=70\%$) sizes at the start of each simulation. For the marine and polar low and high wind speed cases, the total condensation sink across the complete aerosol concentration for is given in Table 2b, also for wet and dry sizes.

For each maritime and polar maritime case, simulations using binary nucleation were conducted for meteorological conditions corresponding to horizontal advection without adiabatic cooling, adiabatic cooling of an air parcel, adiabatic cooling of an air parcel with small scale turbulent fluctuations, and adiabatic cooling followed by entrainment of free tropospheric air during multiple cycles through the boundary layer. For cases under which nucleation is not encountered, sensitivity studies are conducted to determine what changes could lead to nucleation. Finally, simulations are conducted using the new ternary nucleation theory [Korhonen *et al.*, 1999] for all polar maritime and maritime cases for adiabatic cooling.

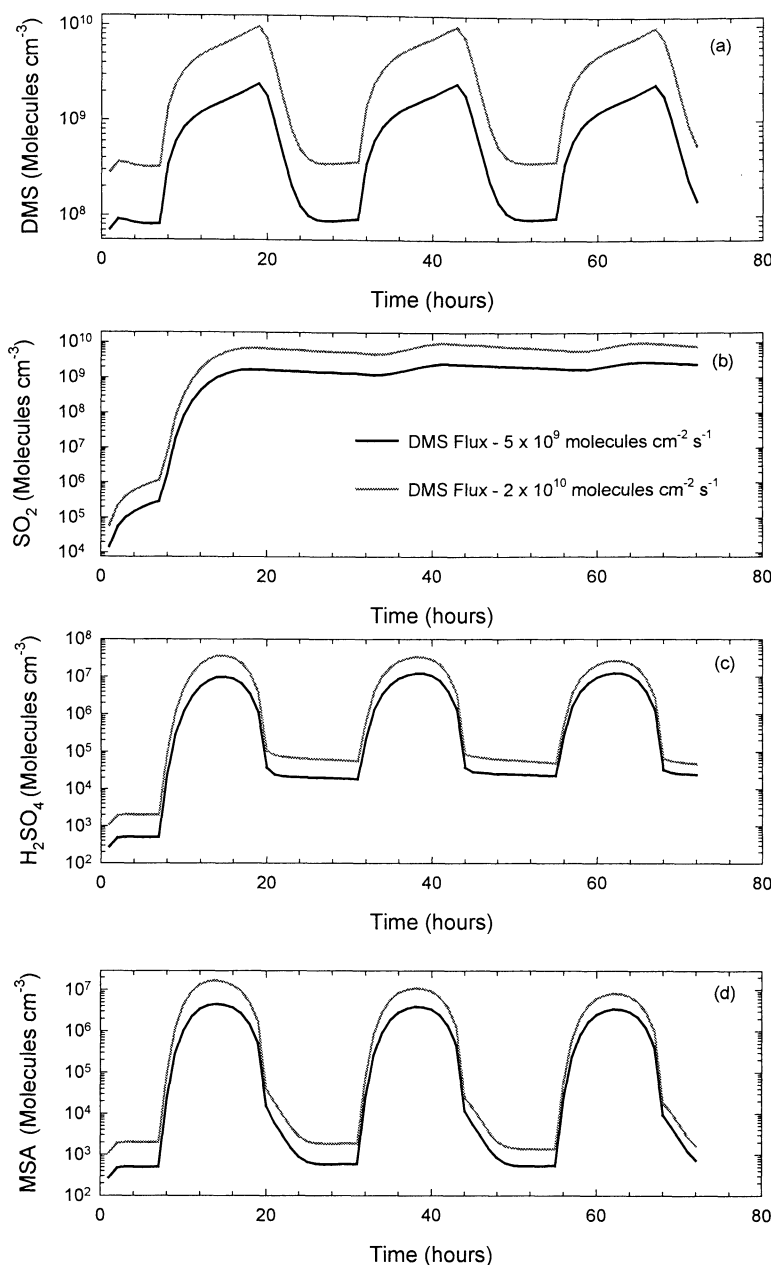


Figure 1. Time evolution of (a) DMS, (b) SO_2 , (c) H_2SO_4 , and (d) MSA with high and moderately low DMS fluxes.

4. Results

4.1. Horizontal Advection

Initial conditions for horizontal advection simply correspond to advection at the 10 m height without any changes in either T or RH. Simulations for this scenario indicate that no binary nucleation occurs for any of the marine or polar marine cases. It should be noted that, in this study, we choose to define particle formation at a certain size as when the concentration at that size is increased more than 10%. For 1 nm sizes, although an increase in concentration of less than 10% is, strictly speaking, nucleation, it is not, however, deemed significant. In the following discussion, unless concentrations increase by more than 10%, particle formation is said not to occur. N_{tot} is defined as the total particle concentration at sizes larger than 1 nm and includes stable new particle embryos, while N_3 corresponds to detectable-

size particle concentration as reported in previous experimental studies. N_3 concentrations are compared to field observations of new particle formation.

4.2. Adiabatic Cooling

Letting the air parcel rise adiabatically from the surface in the MBL results in a dry lapse rate of $9.6 \text{ }^\circ\text{C km}^{-1}$. Decreasing T causes RH to increase, reaching 99% at a height of about 600 m, after which the air parcel is forced to sink back down to the surface. The boundary layer inversion is constrained, not unrealistically, to occur at 600 m in order to avoid cloud formation. To provide a high cooling rate, the updraft velocity is set to 1 m s^{-1} , resulting in a timescale of 18 min for a full boundary layer circulation with the air parcel rising from the surface to the inversion level and back to the surface again. Initial concentrations of the gases were taken from Figure 1 at 15

Table 1. Aerosol and Meteorological Initial Conditions for Polar Maritime and Maritime Air Masses

Type	Maritime				Polar Maritime			
	MI	MII	MIII	MIV	PI	PII	PIII	PIV
T , °C	10	10	10	10	-3	-3	-3	-3
RH, %	70	70	70	70	70	70	70	70
Wind speed, m s ⁻¹	4	4	16	16	2	2	10	10
DMS flux, cm ⁻² s ⁻¹	5 × 10 ⁹	2 × 10 ¹⁰	5 × 10 ⁹	2 × 10 ¹⁰	5 × 10 ⁹	2 × 10 ¹⁰	5 × 10 ⁹	2 × 10 ¹⁰
DMS, ppt	100	400	100	400	100	400	100	400
N_{tot} , cm ⁻³	400	400	400	400	385	385	385	385
d_{tot} , nm	50	50	50	50	40	40	40	40
σ_{tot}	1.4	1.4	1.4	1.4	1.4	1.4	1.4	1.4
N_{acc} , cm ⁻³	100	100	100	100	10	10	10	10
d_{acc} , nm	150	150	150	150	140	140	140	140
σ_{acc}	1.45	1.45	1.45	1.45	1.45	1.45	1.45	1.45
N_{film} , cm ⁻³	4.6	4.6	63.5	63.5	2.97	2.97	17.1	17.1
d_{film} , nm	200	200	200	200	200	200	200	200
σ_{film}	1.9	1.9	1.9	1.9	1.9	1.9	1.9	1.9
N_{jet} , cm ⁻³	0.76	0.76	2.4	2.4	0.63	0.63	1.36	1.36
d_{jet} , nm	2000	2000	2000	2000	2000	2000	2000	2000
σ_{jet}	2.0	2.0	2.0	2.0	2.0	2.0	2.0	2.0

hours from the start (midnight) of the simulation when sulphuric acid has its maximum (1.3×10^7 and 2.7×10^7 molecules cm⁻³). The time evolution of T and RH for these meteorological conditions are illustrated in Figure 2a.

The results of these Lagrangian simulations with adiabatic cooling indicate that no nucleation is observed in the marine cases; however, for polar air, adiabatic cooling combined with extreme conditions (types PII and PIV) of high DMS fluxes, low temperature and high relative humidity, moderate nucleation was observed for both the low and high wind speed cases. Figure 2b illustrates the time evolution of total and detectable particle concentrations for a full boundary layer circulation for PII (i.e. low wind speed and high DMS flux) where it is seen that the initial particle number concentration increased from 397 cm⁻³ to 682 cm⁻³ (N_{tot}); however, almost none (1%) of the newly formed particles had enough time to grow to detectable sizes with diameters greater than 3 nm (N_3). If the simulation is allowed to run for 10 cycles, or boundary layer circulations, then after this period, N_{tot} increased to 12,250 cm⁻³ and N_3 increased to 11,610 cm⁻³ (Figure 3a). The initial sulphuric acid concentration of 3×10^7 molecules cm⁻³ increased to a peak values of 9.5×10^7 molecules cm⁻³ after approximately 50 min. Thereafter, it declined due to the increased condensation sink associated with the newly formed particles.

For the higher wind speed and high DMS flux case, PIV, the total particle number concentration (N_{tot}) was enhanced from 412 cm⁻³ to 528 cm⁻³ and no enhancement was observed for N_3 after one cycle. After 10 cycles, N_{tot} increased to 2,842 cm⁻³ and N_3 increased to 2,097 cm⁻³ (Figure 3b). In this case, due to the greater condensation sink associated with the higher sea-salt concentrations, the peak sulphuric acid concentrations reached a lower value of 6.5×10^7 molecules cm⁻³. For comparison, the

cases PI and PIII, where no nucleation was observed, the peak sulphuric acid concentrations reached were 2.7×10^7 molecules cm⁻³ and 2.9×10^7 molecules cm⁻³, respectively.

4.3. Adiabatic Cooling With Small-Scale Fluctuations

To examine the role of boundary layer dynamics in enhancing nucleation rate, the combined effects of adiabatic cooling and small-scale fluctuations in temperature, water vapor and sulphuric acid concentrations are also investigated. Fluctuations in water vapor and temperature cause fluctuations in relative humidity. As reported by *Easter and Peters* [1994], nucleation rate can be enhanced if the fluctuations in temperature and relative humidity are anticorrelated. *Nilsson et al.* [2000] have shown that mean nucleation rate and net particle concentration are not very sensitive to the fluctuation period, but the most important wave characteristic is the wave amplitude. In this work the fluctuation period is assumed to be 30 s.

The temperature, water vapor and sulphuric acid concentrations are predicted by Monte Carlo simulations with 1000 realizations. T , C_{H_2O} , and C_{SA} are assumed to obey the normal distribution with mean values \bar{T} , $\overline{C_{H_2O}}$, and $\overline{C_{SA}}$, and standard deviations σ_T , σ_{H_2O} , and σ_{SA} . We can write $T = \bar{T} + T'$, $C_{H_2O} = \overline{C_{H_2O}} + C_{H_2O}'$, and $C_{SA} = \overline{C_{SA}} + C_{SA}'$, where T' , C_{H_2O}' , and C_{SA}' are random fluctuations calculated, according to *Sabelfeld* [1991] and *Kulmala et al.* [1997], by the formula (analogous also to H₂O and SA)

$$T' = \sigma_T \sum_{i=1}^l \frac{1}{\sqrt{l}} [\zeta_i \cos(\lambda_i t) + \eta_i \sin(\lambda_i t)]$$

ζ_i and η_i are random numbers sampled according to a normal distribution with zero mean and unit standard deviation, and λ_i is

Table 2a. Normalized Condensation Sink for Marine and Polar Aitken and Accumulation Modes and Sea-Salt Film and Jet Drop Modes

	Condensation Sink, cm ⁻²					
	M_{ait}	P_{ait}	M_{acc}	P_{acc}	Film	Jet
Dry	4.48 × 10 ⁻⁷	2.94 × 10 ⁻⁷	8.20 × 10 ⁻⁷	7.61 × 10 ⁻⁸	6.85 × 10 ⁻⁶	1.19 × 10 ⁻⁴
Wet(70%)	1.12 × 10 ⁻⁶	7.39 × 10 ⁻⁷	7.16 × 10 ⁻⁶	6.45 × 10 ⁻⁶	1.37 × 10 ⁻⁵	2.03 × 10 ⁻⁴

Table 2b. Total Condensation Sink for Marine and Polar High and Low Wind Cases

	Total Condensation Sink cm^{-2}			
	MI	MIII	PI	PIII
Dry	6.52×10^{-4}	1.26×10^{-3}	2.45×10^{-4}	4.30×10^{-4}
Wet(70%)	1.4×10^{-3}	2.5×10^{-3}	0.54×10^{-3}	8.9×10^{-4}

a random value sampled according to the spectral density of the correlation function $f[\lambda]$

$$f(\lambda) = \frac{\sigma_T^2 \tau_c}{\pi (1 + \lambda^2 \tau_c^2)}$$

τ_c is the correlation time for the temperature and assumed to be 2.5 s. The number of harmonics l is chosen to equal 100 which is big enough to give the desired accuracy.

Mean values of temperature, water vapour and sulphuric acid are the same as in the above mentioned adiabatic cooling case, and standard deviations used in this work are 30% of the current mean value for sulphuric acid concentration, 1 K for temperature and 10% of mean water vapor concentration, also values 0.5 K and 5% for water vapor were used. This results in about 5% or 2.5% variations in the mean relative humidity which are in good agreement with observations made at the Mace Head marine monitoring station.

Figure 4 shows the resulting fluctuations encountered in one random Monte Carlo realization of the polar PIII-case (high sea-salt flux, low DMS flux) for a complete boundary layer

circulation. No nucleation was observed again for the marine cases; however, binary nucleation was observed in the least favorable (i.e., highest condensation sink and lowest precursor source rate) of the polar marine cases (due to computational constraints, Monte Carlo simulations were only conducted for the least favorable of the polar cases on the basis that if nucleation was to occur here, then it would occur in all polar cases).

The results of these simulations are illustrated in Figure 5 where the probability of frequency-of-occurrence of the change in total number concentration during the simulations is displayed. The results indicate that in some cases almost 500 new particles per cm^3 could be produced above the background N_{tot} concentration of $\approx 400 \text{ cm}^{-3}$. The mean enhancement in particle concentration is, however, of the order of 103 cm^{-3} , and the peak in occurrence occurs between $60\text{--}70 \text{ cm}^{-3}$. While there is evidence of significant nucleation via binary nucleation with adiabatic cooling and small scale turbulent fluctuations, a maximum of 2% of these particles can grow into detectable sizes after one circulation. Although Monte Carlo simulations were not conducted for 10 circulations of the boundary layer, it does, however, seem likely that, if 2% particles grow to 3 nm sizes

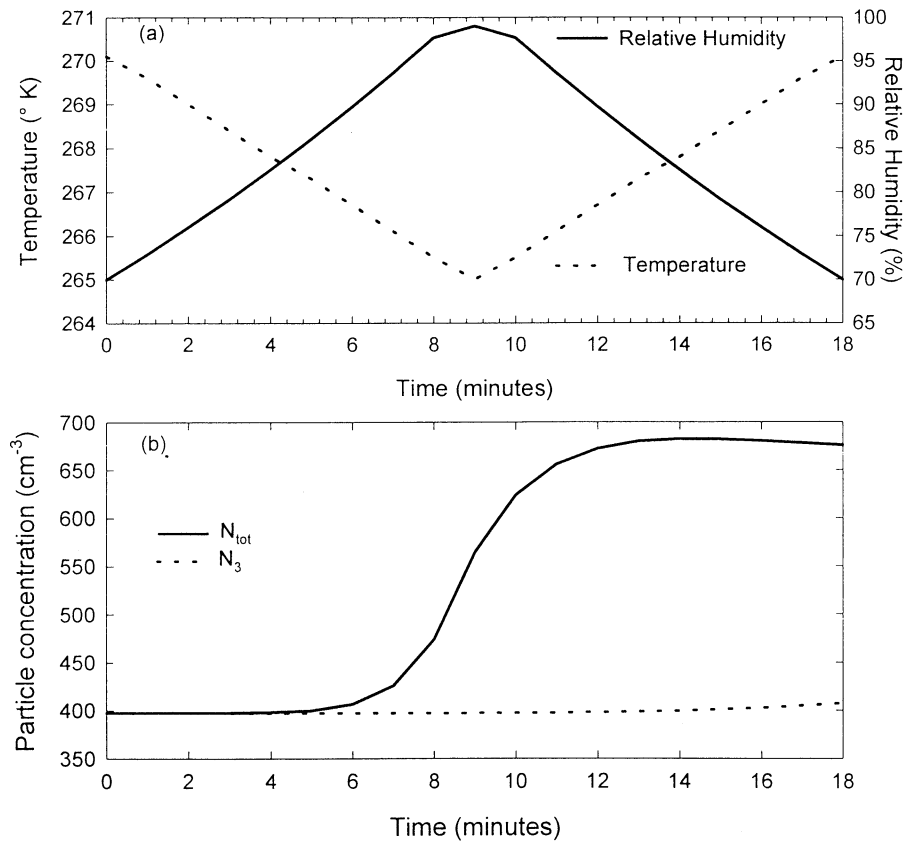


Figure 2. (a) Time evolution of T and RH and (b) total aerosol number concentration (N_{tot}) and number concentration of particles greater than 3 nm in diameter (N_3) when an air parcel rises adiabatically in polar case PII with high DMS flux and low sea salt.

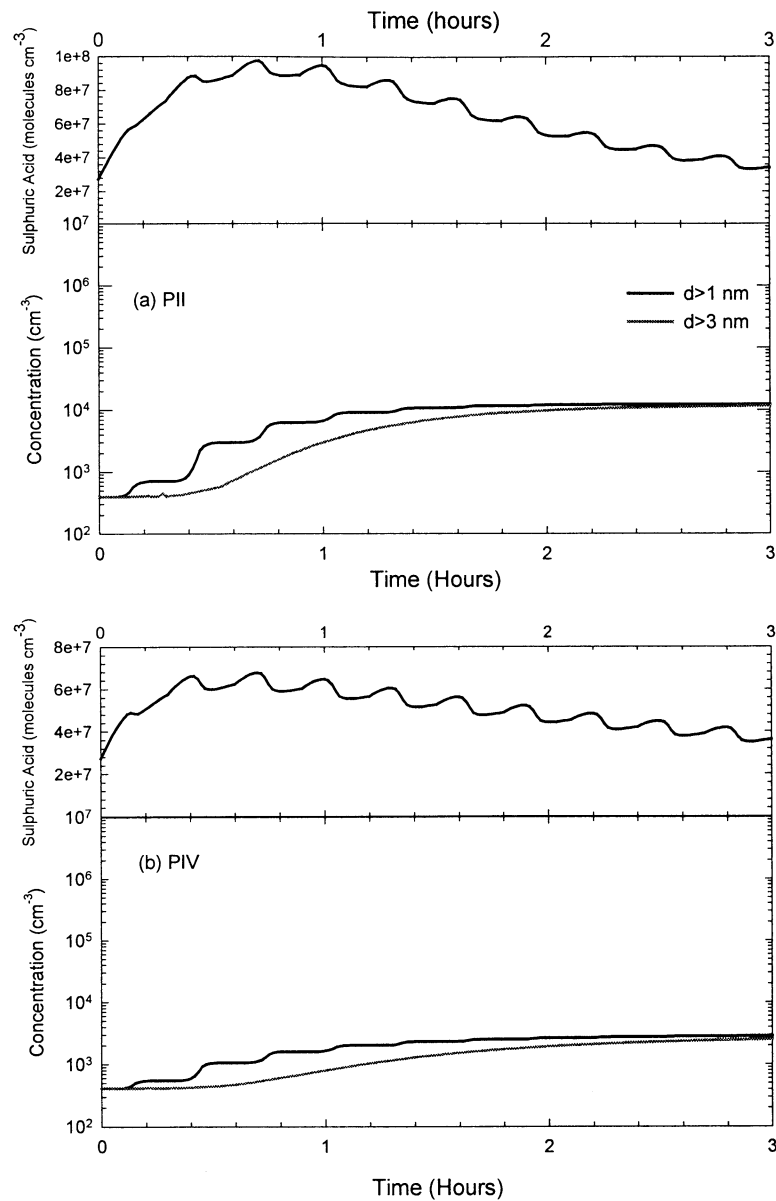


Figure 3. Time evolution of sulphuric acid, N_{tot} , and N_3 for cases PII and PIV after 10 cycles.

after 1 circulation, a significant amount (i.e. >10%) will grow to detectable sizes after 10 circulations.

4.4. Free Troposphere Mixing and Multiple Boundary Layer Cycling

Nilsson and Kulmala [1998] illustrated that nucleation rates are enhanced when mixing of two air parcels comprising different temperatures and humidities occurs. For these simulations we consider a very extreme scenario in which meteorological processes produce conditions with a very low aerosol condensation sink and exceptionally high sulphuric acid concentrations. These exceptional conditions could conceptually occur under conditions of vigorous convection, leading to large precipitating cumulus formation, in regions of high DMS fluxes. In such situations, high concentrations of DMS can be rapidly transported to the free troposphere while preexisting particle concentration can be significantly reduced due to precipitation

scavenging. Once this process occurs, we assume a warm dry free tropospheric layer above the MBL inversion with $T=15$ °C and dryer RH=30%, a low particle concentration with $N_{tot}=10$ cm⁻³, $d=80$ nm, $\sigma=1.45$, and a high sulphuric acid concentration of 1.2×10^8 cm⁻³. Specifically, it can be assumed that another air mass far from the place considered may have originated in an area of very high DMS fluxes and during the transport time, the oxidation of DMS yields high sulphuric acid concentrations. This layer can then be entrained to the cooler and more moist MBL layer with the potential to enhance nucleation probability. A schematic of such a scenario is illustrated in Figure 6.

In these simulations it is assumed that an air parcel (maritime or polar maritime) rises adiabatically to 600 m and mixes with a warmer and dryer free tropospheric air through entrainment and then returns to the surface. This cycle is then repeated 10 times to examine how the aerosol concentration could change over a longer period of time. After entrainment, the average gas and particle concentrations in the air parcel are weighted, according to

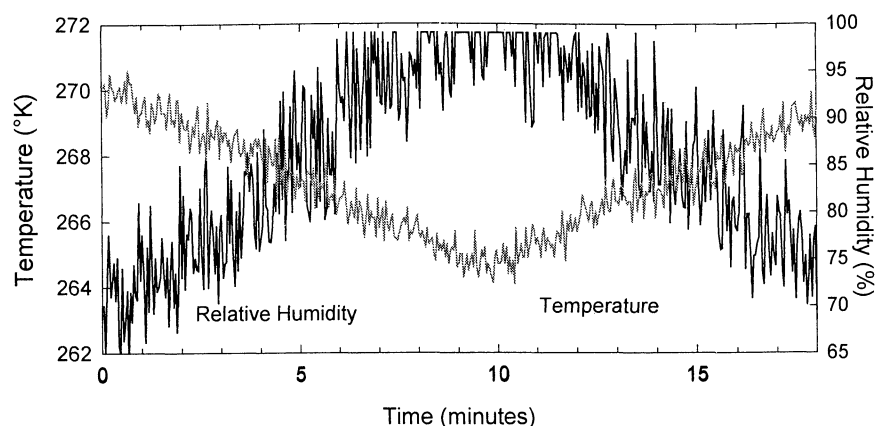


Figure 4. Fluctuations in T and RH in one random Monte Carlo realization of the polar case PIII.

the degree of entrainment, comprising 5%, 10%, or 30% of the inversion layer concentrations and 95%, 90%, and 70%, respectively, of the original air parcel concentrations.

The results of these simulations indicate that, for the maritime case, mixing due to entrainment did not result in nucleation, even when clean air containing a low condensation sink and high sulphuric acid is entrained; however, nucleation is now observed in all polar cases. Additionally, significant enhancement is also seen in detectable particle concentrations (N_3). The temporal evolution of sulphuric acid, total, and detectable particle concentrations is displayed in Figure 7 for polar maritime case PIII with 30% entrainment. For 30% entrainment, sulphuric acid concentrations rise steadily from 1.7×10^7 molecules cm^{-3} to a peak value of 1.2×10^8 , leading to an increase in particle concentrations (after 10 cycles) of 11,840 cm^{-3} and 6,533 cm^{-3} for N_{tot} and N_3 , respectively. Reducing the entrainment rate to 10% in PIII, leads to a very modest enhanced of N_{tot} to 448 cm^{-3} and a reduction in N_3 to 257 cm^{-3} after an initial reduction of total particle concentration due to dilution. Further reduction in entrainment rate to 5% leads to a noticeable reduction in N_{tot} to 289 cm^{-3} and a similar reduction in N_3 to 264 cm^{-3} .

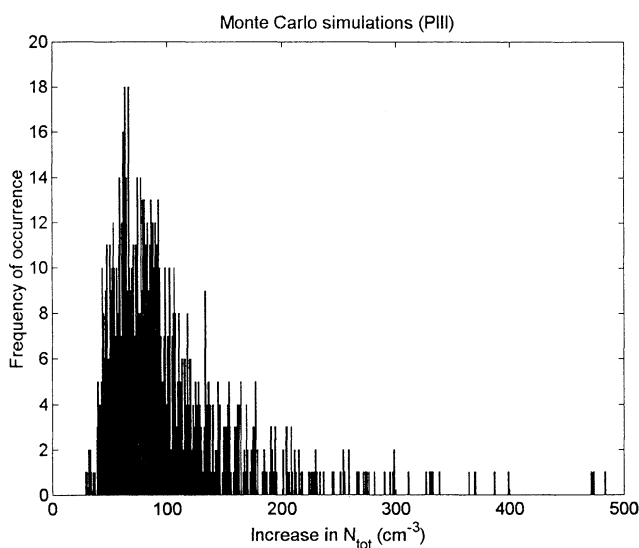


Figure 5. Increase in N_{tot} resulting from Monte Carlo simulations with 1000 realizations in polar case PIII. Mean value and STD for the increase are 102.6 and 61 cm^{-3} , median is 86.4 cm^{-3} .

For the PI case, after 10 such circulations with 30% entrainment in each circulation, N_{tot} increases to 12,120 cm^{-3} , while N_3 increases to 7,462 cm^{-3} . Owing to the high entrainment rates, sulphuric acid concentration approaches 1.2×10^8 molecules cm^{-3} after a few circulations. By comparison, for 10% entrainment, N_{tot} and N_3 increase to 1,254 cm^{-3} and 698 cm^{-3} respectively, with sulphuric acid vapor concentrations reaching 6.5×10^7 molecules cm^{-3} ; for 5% entrainment, N_{tot} increases to 484 cm^{-3} , however, N_3 reduces to 361 cm^{-3} due to dilution effects with the cleaner free tropospheric air while sulphuric acid reaches 4.1×10^7 molecules cm^{-3} .

4.5. Threshold Aerosol Conditions for Binary Nucleation

For the conditions that did not lead to nucleation, it is useful to explore what changes in aerosol concentrations and temperature can trigger nucleation. Changes in relative humidity are not examined since surface level (i.e., 10 m) relative humidity is rarely less than 70% and, in the absence of cloud, relative humidity can not be greater than 99–100%. Constraining the relative humidity profile to this range leaves three variables that can influence nucleation: temperature, the aerosol condensation sink and the source rates of the precursor gas, sulphuric acid in this case. As illustrated earlier in the polar cases, the lower the temperature is, the more probable nucleation is. For a given temperature the probability of nucleation occurring is directly related to the balance between the source rate of the vapor precursor and its loss rate through heterogeneous or homogeneous nucleation. Heterogeneous nucleation loss is primarily related to the rate of condensation to the preexisting aerosol, the so-called condensation sink.

Since we are, however, dealing with a dynamic situation where the condensation sink is continuously varying due to boundary layer circulations and the condensation sink affects particle production in three ways, determining a threshold condensation sink that promotes nucleation is difficult to summarise into one term. For example, the condensation sink will determine the peak vapor supersaturation reached before nucleation; it will determine the rate of growth of stable embryos to new 3 nm particles-sizes, and also, it will influence the scavenging of the new stable embryos. The latter two processes are competing processes leading to new particle occurrence. Notwithstanding this difficulty, it is still useful to report at least the dry-size condensation sink associated with the preexisting aerosol since this can be readily converted to its wet size using Kohler theory. It should be noted that the condensation sink is not directly related to surface area and should not be confused with being

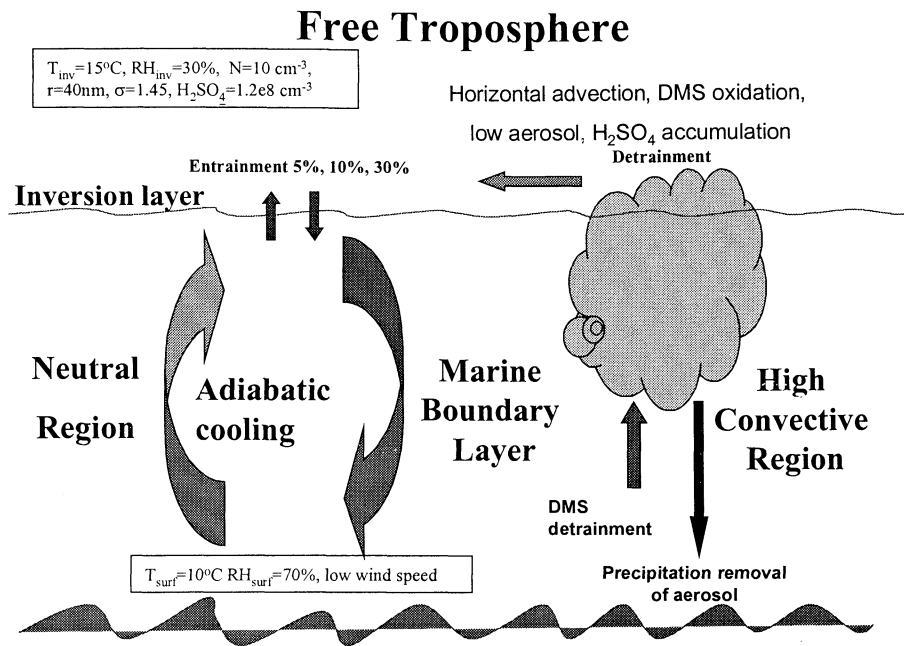


Figure 6. Schematic picture of entrainment with a warmer and cleaner inversion layer.

related to the condensation rate of gas phase species to the preexisting aerosol. Following *Fuchs and Sutugin* [1970], for Aitken mode sizes (i.e. the molecular regime), the condensation sink is proportional to d^2 and for the largest sizes (i.e. the continuum regime), condensation is proportional to d while in the intermediate transition regime, condensation is proportional to d^n where n is between 1 and 2 [Also see *Pirjola et al.*, 1999]. Consequently, as a result of deriving condensation sinks based on aerosol surface area, large errors emerge at sizes greater than 100 nm. For the Aitken, accumulation, film, and jet drop modes, their respective normalized dry-size condensation sinks are $CS_{Ait}=4.48 \times 10^{-7}\text{ cm}^{-2}$, $CS_{Acc}=8.2 \times 10^{-5}\text{ cm}^{-2}$, $CS_{film}=6.85 \times 10^{-6}\text{ cm}^{-2}$, and $CS_{jet}=1.19 \times 10^{-4}\text{ cm}^{-2}$. For each of the cases presented

previously, their respective integrated condensation sink for the given concentrations and at the initial relative humidity of 70% are $CS_{MI, MIV}=1.4 \times 10^{-3}\text{ cm}^{-2}$, $CS_{MIII, MIV}=2.5 \times 10^{-3}\text{ cm}^{-2}$, $CS_{PI, PIV}=5.4 \times 10^{-4}\text{ cm}^{-2}$, and $CS_{PIII, PIV}=8.9 \times 10^{-4}\text{ cm}^{-2}$. In the marine cases the sea-salt modes contribute to between 10% and 53% of the condensation sink (depending on wind speed), while for the polar case, the sea-salt contribution is of the order of 15-75%.

The condensation sink increases with increasing humidity as particle sizes grow through water condensation. For example, ammonium sulphate Aitken mode particles grow to 1.6 times their dry size at a relative humidity of 90% while accumulation mode particles grow to 1.8 times the dry size. Sea-salt particles undergo a larger growth-factor change to 2.3 under similar

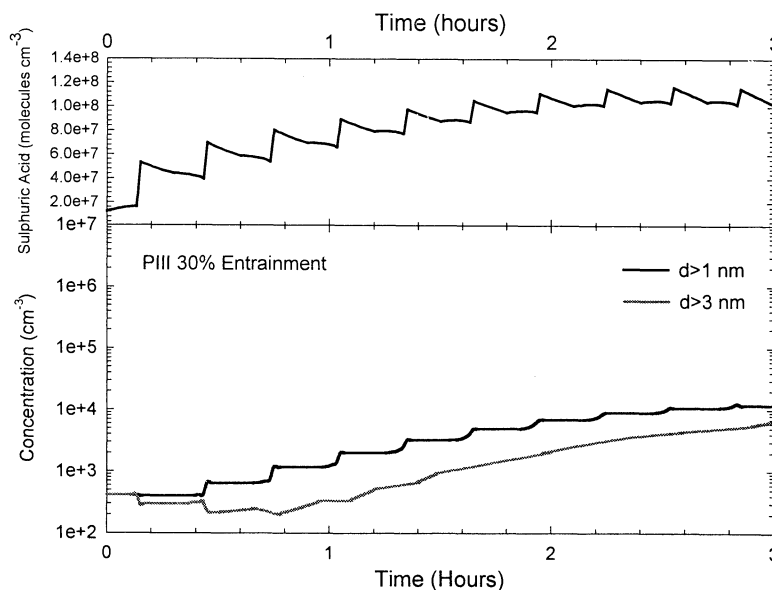


Figure 7. Sulphuric acid concentration, N_{tot} and N_3 in multiple boundary layer cycling in polar case PIII with 30% entrainment.

Table 3. Probability for Nucleation (Change in N_{tot})^a

Lagrangian, Horizontal	Adiabatic Cooling [AC]	AC+Fluctuations	AC+Mixing /Cycles	Ternary Nucleation
M1	–	–	–	+
MII	–	–	–	+ ^b
MIII	–	–	–	+
MIV	–	–	–	+ ^b
PI	–	+ ^b	+ ^b	+ ^b
PII	+ ^b	+ ^b	+ ^b	+ ^b
PIII	–	+ ^b	+ ^b	+ ^b
PIV	+ ^b	+ ^b	+ ^b	+ ^b

^anegative means no nucleation; positive means nucleation (N_{tot} increases).

^bcorresponds to particle production in detectable size (N_3).

humidity conditions (K. Hämeri, personal communication, 2000). At relative humidities of 99% the growth factor is almost double that at 90%. As a parcel undergoes boundary layer circulations, the condensation sink at the boundary layer top (relative humidity=99%) is ≈ 10 higher than at the surface for the Aitken mode; ≈ 6 time higher for the accumulation mode; 5 times for the film mode; and 4 times for the jet drop mode, thus highlighting the no-linear relationship between condensation sink and relative humidity. Given the above arguments, only variations in the dry condensation sink are examined in order to promote nucleation.

Since no nucleation was observed in any of the horizontal advection cases, the initial aerosol concentration is reduced to a level where nucleation occurs for surface-level air. In the marine cases, if the concentration in each mode is reduced by a factor of 10, leading to a condensation sink of $1.4 \times 10^{-4} \text{ cm}^2$ and a vapor source rate (i.e., the product of C_{OH} times C_{SO_2}) of $0.81\text{--}3.65 \times 10^4 \text{ molecules m}^{-3} \text{ s}^{-1}$, nucleation is still not observed. Either the concentration of particles has to be reduced further by a factor of 10, or the 10 m temperature has to be decreased by $> 10^\circ\text{C}$ in addition to the initial factor of 10 reduction in concentration before nucleation becomes probable. If the concentration is not reduced, then a reduction in temperature of the order of 30°C is required to produce nucleation.

This is in good agreement with the predictions of significant particle production as a function of condensation sink and sulphuric acid source rate previously examined Pirjola *et al.* [1999]. In the Pirjola *et al.* [1999], study, a full sensitivity study of the dependence of particle production on vapor source rate, condensation sink, relative humidity, and temperature can be found. Reducing particle concentration by 10 results in a total particle concentration of the order of 55 cm^{-3} , which may be reasonable after extensive precipitation. This reduction corresponds to an Aitken mode concentration of 40 cm^{-3} and an accumulation and film mode concentration of 15 cm^{-3} . However, particle concentrations of the order of 5 cm^{-3} (4 Aitken and 1 accumulation mode) are very rarely encountered in marine air. On the other hand, temperature reductions of 10° , combined with a factor of 10 reduction in concentration is more likely to induce nucleation. By comparison, in polar air, reducing the concentration by 10 leads to a vapor source rate of $3.99 \times 10^3 \text{ cm}^{-3} \text{ s}^{-1}$ (PI, PIII) and $2.96 \times 10^4 \text{ cm}^{-3} \text{ s}^{-1}$ (PII, PIV) and condensation sinks of 5.4×10^{-5} (PI, PII) and $8.9 \times 10^{-5} \text{ cm}^2$ (PIII, PIV). For these situations, nucleation is produced for all but the PIII case (i.e., low DMS flux, high sea-salt flux). It should be noted, however, that the sulphuric acid concentration for PII and PIV are excessively high (greater than $2 \times 10^8 \text{ molecules cm}^{-3}$) and are probably not realistic. The Aitken mode concentration in this scenario is 38 cm^{-3} , while combined accumulation and film mode aerosol concentration is $1.3\text{--}2.7 \text{ cm}^{-3}$. For the marine-case

adiabatic cooling simulations that resulted in no nucleation, reducing the concentration by a factor of 10 only led to nucleation for MII and MIV (i.e. the high DMS flux cases). For these simulations, nucleation is predicted for sulphuric acid source rates of $3.4 \times 10^4 \text{ cm}^{-3} \text{ s}^{-1}$ and for a condensation sink of $2.5 \times 10^{-4} \text{ cm}^2$, while no nucleation is observed for a source rate of $9.66 \times 10^3 \text{ cm}^{-3} \text{ s}^{-1}$ and a condensation sink of $1.4 \times 10^{-4} \text{ cm}^2$. The factor of 10 reduction in MII concentration leads to the production of $1000 \text{ cm}^{-3} N_3$ particles after about 2 hours, while in the MIV case, N_3 increases only to 300 cm^{-3} particles over the same time period.

4.6. Ternary Nucleation

The recent advances in ternary nucleation theory [Korhonen *et al.*, 1999] allows us to test, for the first time, whether or not ternary nucleation can produce new particles in the MBL and also lead to an enhancement in the detectable particle concentration. Taking an ammonia concentration of 5 ppt, simulations under adiabatic cooling conditions lead to ternary nucleation occurring for all conditions considered. For the case with high sea-salt flux and low DMS flux, MIII, nucleation of $50,000 \text{ cm}^{-3}$ was seen after the first cycle (Figure 8), occurring for a sulphuric acid concentration of $1.27 \times 10^7 \text{ molecules cm}^{-3}$. Thereafter, sulphuric acid concentration reduces to between $5\text{--}7 \times 10^6 \text{ molecules cm}^{-3}$ for the duration of the simulation. A small amount of nucleation is seen for each cycle for these acid concentrations, and a minor enhancement of $40 \text{ particles cm}^{-3}$ in N_3 is seen after 3 hours, while the majority of N_{tot} gradually decays due to coagulation losses. By comparison, for the case with low sea-salt and high DMS (MII), an initial sulphuric acid concentration of $3 \times 10^7 \text{ molecules cm}^{-3}$ was observed, leading to nucleation of more than $10^7 \text{ particles cm}^{-3}$. Sudden depletion of the acid vapor resulted after nucleation, and thereafter, this vapor concentration rapidly recovered to a level between 8×10^6 and $2.4 \times 10^7 \text{ molecules cm}^{-3}$ for the duration of the simulation (3 hours). This persistent high concentration of sulphuric acid nucleated particles again on every cycle and provided enough condensable mass to grow almost 10^5 particles cm^{-3} to 3 nm sizes.

An additional case (M0) was simulated which predicts particle formation for a case similar to M1 (i.e. low sea-salt flux) but with a lower DMS flux leading to peak values of 20 ppt as opposed to 100 ppt and 400 ppt in cases MII and MIII, respectively. In this case, illustrated in Figure 9, an initial sulphuric acid concentration of $3.1 \times 10^6 \text{ molecules cm}^{-3}$ leads to nucleation of more than $10^4 \text{ particles cm}^{-3}$, after which the sulphuric acid concentration decreases to $2.3 \times 10^6 \text{ molecules cm}^{-3}$ and then oscillates between $1.8\text{--}2.4 \times 10^6 \text{ molecules}$ for the duration of the simulation. It should be noted that initial simulations for this case

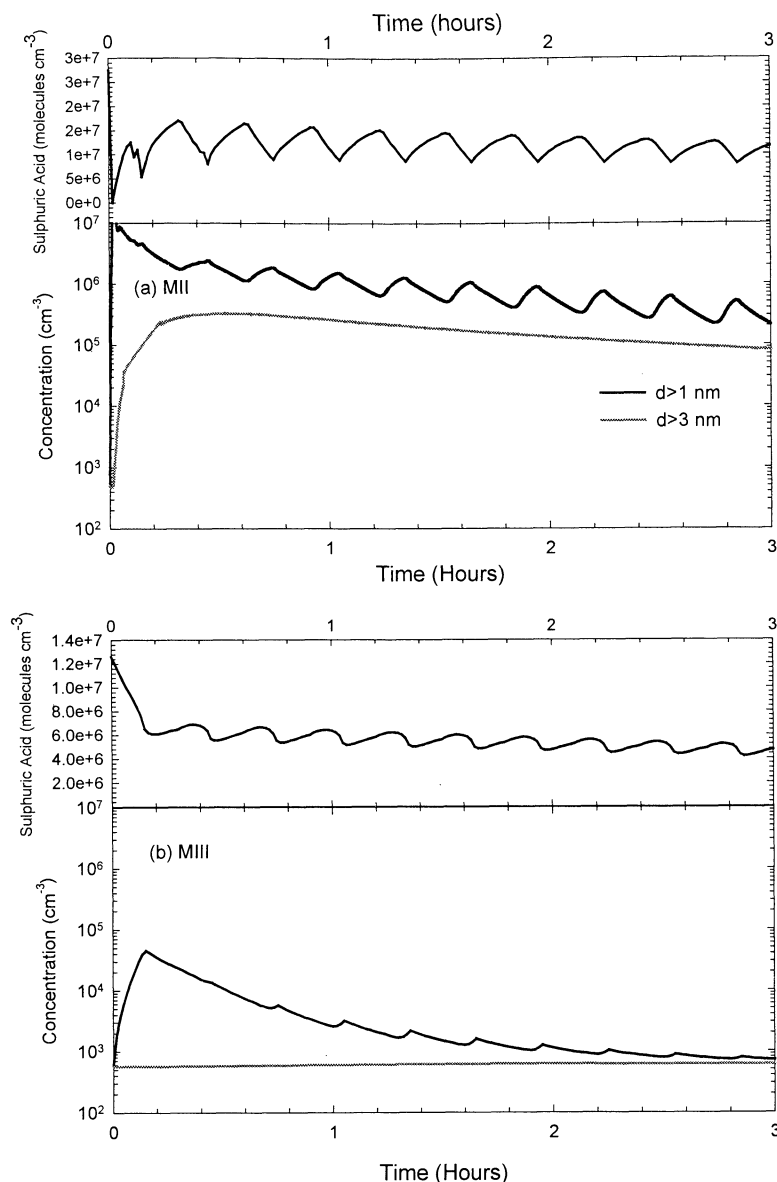


Figure 8. Time evolution of N_{tot} and N_3 under adiabatic cooling conditions for cases MII and MIII with ammonia concentration of 5 ppt and with ternary H_2SO_4 - H_2O - NH_3 nucleation mechanism.

(M0), no nucleation was observed due to the low level of ammonia (5 ppt) and, consequently, ammonia was increased to 70 ppt. While nucleation is seen in all cycles for this range of sulphuric acid and ammonia concentrations, there is insufficient condensable vapor available to grow the new particles to 3 nm sizes, and the total concentration decays back to initial background concentrations due to coagulation losses. In summary, for ternary nucleation to lead to a significant production of detectable particles, sustained sulphuric acid, or condensable vapor, concentrations of the order of 10^7 molecules cm^{-3} are required for a number of hours. Sensitivity studies on factors influencing ternary nucleation rates are discussed in more detail by Korhonen *et al.* [1999] while factors influencing growth to 3 nm sizes are discussed, from a generic perspective, by Kulmala *et al.*, [2000].

5. Discussion

Under four tested maritime-case conditions, binary nucleation of sulphuric acid and water is not predicted under typical aerosol

concentrations due to insufficient acid vapor under the given temperature and condensation sink conditions. By comparison, in polar marine air, due to the lower temperatures and lower condensation sinks, nucleation is predicted to occur under conditions with adiabatic cooling and DMS fluxes leading to DMS concentrations of the order of 400 ppt for both low wind (PII) and high wind (PIV) conditions. The sulphuric acid vapor concentration required to produce $\approx 11,000$ cm^{-3} particles in PII (low sea-salt, high DMS) and ≈ 2500 cm^{-3} in PIV (high sea-salt high DMS) is $\approx 9.5 \times 10^7$ molecules cm^{-3} and $\approx 6.5 \times 10^7$ molecules cm^{-3} , respectively. While nucleation was not observed in cases PI and PII for simple adiabatic cooling for sulphuric acid concentrations of 2.7×10^7 molecules cm^{-3} and 2.9×10^7 molecules cm^{-3} , respectively, when turbulent fluctuations were applied to temperature, relative humidity, and sulphuric acid concentrations, nucleation was then predicted for these cases.

In marine air, lowering the particle concentration by a factor of 10 (leading to a total particle concentration of ≈ 50 cm^{-3}) will lead to nucleation under adiabatic cooling conditions and high DMS

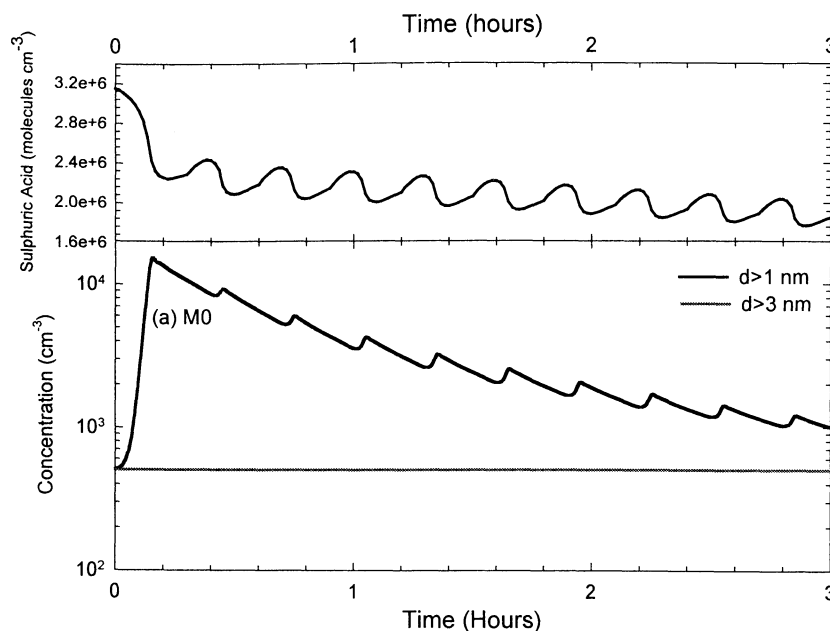


Figure 9. Time evolution of N_{tot} and N_3 under adiabatic cooling conditions for cases M0 with ammonia concentration of 70 ppt and with ternary $\text{H}_2\text{SO}_4\text{-H}_2\text{O-NH}_3$ nucleation mechanism.

fluxes, a while lowering the particle concentration by a factor of 100 is required to induce nucleation under near-surface and horizontal advection conditions. Nucleation is also promoted by a 10°C temperature reduction combined with a ten-fold reduction in particle concentration. In the polar air, reducing the concentration by 10 leads to nucleation in low DMS and sea-salt flux, whereas nucleation did not occur under standard conditions, however, the low condensation sink ($0.54 \times 10^{-4} \text{ cm}^{-2}$) leads to an unusually high sulphuric concentration of $> 2 \times 10^8$ molecules cm^{-3} .

When entrainment of free tropospheric air containing very low aerosol condensation sinks and very high sulphuric acid concentrations (1.2×10^8 molecules cm^{-3}) is considered, nucleation was not predicted in any of the marine cases, but was predicted in all of the polar cases. The strongest nucleation was predicted for high entrainment rates of 30% free tropospheric air into the boundary layer parcel. After multiple entrainment cycles for case PIII, sulphuric acid vapor concentration rises to $\approx 1 \times 10^8$ molecules cm^{-3} after 5 cycles, leading to an enhancement of $\approx 1000 \text{ cm}^{-3}$ particles in N_3 , and after 10 cycles, reaches a steady state concentration of $\approx 1.2 \times 10^8$ molecules cm^{-3} , resulting in an enhancement of $\approx 6000 \text{ cm}^{-3}$ particles in N_3 sizes. By comparison, for low DMS and sea-salt concentrations (PI) and 10% entrainment, a sulphuric acid concentration of 6.5×10^7 molecules cm^{-3} lead to a modest enhancement of $\approx 700 \text{ cm}^{-3}$ N_3 particles.

Field observations of new particle formation in polar marine air masses indicated that N_3 was observed to be enhanced by $\approx 2000\text{-}5000 \text{ cm}^{-3}$ [O'Dowd *et al.*, 1997a] in the regions where highest DMS concentrations of 100-400 ppt occurred [Davison *et al.*, 1996]. Within the same polar air masses, the ammonium-to-sulphate ratio was observed to be near zero [O'Dowd *et al.*, 1997a], suggesting a lack of ammonia within these polar air masses and pointing to binary nucleation as being the most likely nucleation mechanism leading to the observed particle production. While the aforementioned simulations seem to support hypothesis that binary nucleation produced the observed particle concentration enhancement, the likelihood of these conditions occurring must be scrutinised. It should be noted that

DMS concentrations of 100-400 ppt were peak concentrations observed by Davison *et al.*, [1996] and are in very good agreement with the peak concentrations of 100-500 ppt observed by Berresheim *et al.* [1998] on the Sulphur Chemistry in the Antarctic Tropospheric Experiment (SCATE) campaign. More typically, concentrations fall below the 100 ppt level. During the Davison *et al.*, [1996] cruise, no sulphuric acid measurements were available, but during SCATE, Jefferson *et al.* [1998] report sulphuric acid concentrations of the order of 6.5×10^6 molecules cm^{-3} for DMS concentrations < 200 ppt. The reported acid concentrations are an order of magnitude lower than those required by the model simulations to produce, by binary nucleation, an enhancement in N_3 concentrations of the order of $1,000 \text{ cm}^{-3}$. However, from the SCATE measurements, it is not clear what sulphuric acid concentration occurred for the peak DMS concentrations of 500 ppt. A simple scaling of peak acid concentrations to peak DMS concentrations suggest that concentrations approaching 6.5×10^7 molecules cm^{-3} may be possible. To produce enhancements in N_3 of the order of $10,000 \text{ cm}^{-3}$ from binary nucleation, extreme conditions of entrainment resulting in sulphuric acid concentrations of $> 10^8$ molecules cm^{-3} must occur, which, taking the SCATE measurements in account, seem unlikely.

In terms of nucleation in the marine boundary layer, only ternary nucleation of sulphuric acid, ammonia and water can produce new particles. The simulation results in this study suggest that significant nucleation ($> 10^4 \text{ cm}^{-3}$) of new particles will occur for ammonia concentrations of 70 ppt and sulphuric acid concentrations of 3.2×10^6 molecules cm^{-3} , resulting from DMS concentrations of 20 ppt, however, no growth into sizes larger than 3 nm is predicted. For higher DMS concentrations of 100 ppt, and initial sulphuric acid concentrations of 1.2×10^7 molecules cm^{-3} , nucleation of 50,000 particles cm^{-3} is predicted. After the nucleation event, less than 50 particles cm^{-3} can grow to detectable sizes providing the sulphuric acid concentration remains between $5\text{-}7 \times 10^6$ molecules cm^{-3} for the following 3 hours. Although this enhancement of 50 particles cm^{-3} at sizes > 3 nm is less than 10% of the N_3 concentration, this scenario probably represents the threshold condition for ternary nucleation

producing particles in the marine boundary layer. For conditions of very high DMS concentrations (400 ppt) and low aerosol condensation sinks, an initial sulphuric acid concentration of 3×10^7 molecules cm^{-3} produces 10^7 cm^{-3} new particles at the start of the simulation, leading to a final N_3 concentration of 10^5 cm^{-3} if the acid vapor concentration is maintained between $5\text{--}25 \times 10^6$ molecules cm^{-3} for 3 hours of the simulation.

The reported tropical MBL nucleation case observed by *Clarke et al.* [1998], in which N_3 was observed to increase to $>30,000 \text{ cm}^{-3}$, occurred under exceptionally low surface area concentrations, high DMS fluxes (4×10^9 molecules $\text{cm}^{-2} \text{ s}^{-1}$), DMS concentrations of 70–90 ppt, and sulphuric acid concentrations of $2\text{--}5 \times 10^7$ molecules cm^{-3} . Given the above model simulations, it is plausible that this event could be explained by ternary nucleation, and the subsequent growth of new particles produced from DMS oxidation products. By comparison, under more typical environmental conditions, the coastal nucleation bursts with $N_3 > 500,000 \text{ cm}^{-3}$, observed by *O'Dowd et al.*, [1999c] in mid latitude marine air masses cannot be explained by such processes. They concluded that while ternary nucleation was likely to produce new particles, there was insufficient sulphuric acid vapor available to condense and grow these new particles to detectable sizes and that an additional species was required to produce detectable sizes. More recent modeling studies of particle formation and growth corroborate this conclusion and suggest that ternary nucleation of sulphuric acid, ammonia, and water is required to form thermodynamically stable clusters which, thereafter, can grow to detectable sizes by condensation of additional species [*Kulmala et al.*, 2000].

The model simulations presented here do, however, suggest that there may exist a slow, barely detectable, particle production rate providing DMS concentrations are of the order of 100 ppt or above. Measurements, however, indicated that DMS concentrations of this magnitude are more typical of peak DMS concentrations rather than a mean values. Given a more typical general concentration of DMS in the MBL of the order of 20–50 ppt or less, it seems that, while nucleation may occur, significant particle production due to oxidation products from DMS alone will not occur, except under irregular or sporadic circumstances. These sporadic circumstances, due to their infrequency and limited spatial scales, are unlikely to contribute significantly to the background MBL aerosol population.

These simulations also indicate that sea-salt aerosol can provide a controlling influence on the production of new particles since it provides a very important condensation sink in the MBL [*O'Dowd et al.*, 1997b]. Only when the DMS flux is high and the sea-salt flux low, does noticeable particle production occur in the MBL. Since both the flux of DMS and sea salt are directly related to wind speed, the chances of this occurring are quite low. One exception is, as mentioned earlier, under conditions where precipitation removed the preexisting aerosol while leaving most of the DMS suspended in the MBL, will conditions be favorable.

In the above simulations the question of particle production in clouds has not been addressed as all simulations were constrained to simulate particle production in the cloud-free MBL. Some observations of total particle concentration in cloud indicate enhanced concentrations in the upper regions of stratiform clouds [*Hegg et al.*, 1990]. In a subsequent modelling study, *Hegg* [1991] concluded that enhanced actinic radiative flux in the upper regions of stratiform clouds could lead to a sufficient source of sulphuric acid to overcome the enhanced condensation sink encountered in cloud, and consequently reach the supersaturation required for binary nucleation. However, in that study, model simulations of up to 4 hours were required to reproduce the observations of enhanced particle concentration in cloud. It is not very realistic for any parcel of air to remain in cloud for than length of time, thus making this an unlikely explanation for observed CN enhancement. Additionally, recent modelling

studies of heterogeneous sulphate production in marine stratiform clouds [*O'Dowd et al.*, 2000] illustrated that for clean marine conditions, with SO_2 concentrations of 100 ppt, approximately all of the SO_2 was dissolved into cloud droplets, consequently, regardless of enhanced actinic flux, it is unlikely that sufficient sulphuric acid could be produced to promote in-cloud nucleation. Similarly, there have been observations of enhanced CN concentrations around marine cumuli by *Radke and Hobbs* [1991]. On the basis of timescales, the results of the simulations in this study suggest that it is also unlikely for new particles to grow to detectable sizes in cloud outflow in the MBL, particularly since a significant amount of both sulphuric acid, and its precursor SO_2 will be depleted, thus significantly reducing the growth rate of new particles. In summary, inclusion of cloud fields into this analysis is not expected to promote MBL nucleation, but is expected to further inhibit nucleation and growth probability. Despite this, if clouds are precipitating, they can lead to a net removal of a significant fraction of the preexisting aerosol and consequently lead to a lowering of the aerosol condensation sink thereafter. In the marine case, if 90% of the aerosol is removed, then only for the maximum DMS flux values, and an aerosol condensation sink of the order of $2.5 \times 10^{-4} \text{ cm}^{-2}$, is binary nucleation promoted under adiabatic cooling conditions. This situation corresponds to an Aitken mode concentration of 40 cm^{-3} and an accumulation mode of 10 cm^{-3} . Since enhanced DMS flux is also associated with enhanced sea-salt flux, sulphuric acid concentration is unlikely to reach the values required for binary nucleation (i.e. $>10^8 \text{ cm}^{-3}$), however, it is more likely to reach concentrations required for ternary nucleation (i.e. $>10^7 \text{ cm}^{-3}$). Therefore, it is likely that, after aerosol removal through precipitation, the marine boundary layer aerosol may be replenished by ternary nucleation, but not by binary nucleation. These results are qualitatively in agreement with the simulations by *Capaldo et al.* [1999], who also illustrated that precipitation removal of preexisting aerosol can promote nucleation, however, they did not find that the frequency of precipitation-related particle production was sufficient to explain the boundary layer concentration. In agreement with the approach used by *Capaldo et al.* [1999], this study confirms that nucleation is most likely to occur at the top of the boundary layer where temperatures are lower and humidity is highest, and not close to the ocean surface.

6. Conclusions

Binary nucleation of the $\text{H}_2\text{SO}_4\text{--H}_2\text{O}$ system is not predicted to occur in the MBL for realistic conditions, regardless of meteorological conditions such as adiabatic cooling, turbulent fluctuations or entrainment. Considering adiabatic cooling leading to boundary layer circulations, only in polar air masses with high DMS fluxes leading to peak DMS concentrations of 400 ppt and sulphuric acid concentrations greater than 4×10^7 molecules cm^{-3} , was nucleation predicted to occur; however, for detectable particles sizes (N_3) to be enhanced, sulphuric acid concentrations greater than $6\text{--}6.5 \times 10^7$ molecules cm^{-3} were required for a timescale of the order of ≈ 3 hours. Turbulent fluctuations were predicted to enhance nucleation occurrence for cases in which nucleation would not otherwise occur (i.e., polar air masses with low DMS flux of high condensation sinks). Entrainment of sulphuric acid – rich free tropospheric air ($>1.2 \times 10^8$ molecules cm^{-3}) with very low aerosol concentrations ($<10 \text{ cm}^{-3}$) led to significant nucleation and N_3 – particle production when entrainment resulted in the accumulation of MBL sulphuric acid concentrations to $6\text{--}12 \times 10^7$ molecules cm^{-3} . Below this sulphuric acid concentration, entrainment resulted in a dilution of MBL aerosol and a net reduction in N_3 particle concentration. Comparison with field measurements of DMS and sulphuric acid concentration in polar air suggest that for realistic boundary layer

concentrations of these species, binary nucleation of sulphuric acid and water could, plausibly, lead to enhancements in detectable particle size concentration of the order of 1000 cm^{-3} , but not to enhancements of the order of $10,000 \text{ cm}^{-3}$.

Ternary nucleation of sulphuric acid, water, and ammonia was predicted to occur for all marine and polar marine scenarios where ammonia concentrations were above 5 ppt and sulphuric acid vapor concentrations above $4 \times 10^6 \text{ molecules cm}^{-3}$, however, detectable particle size (N_3) production only occurred for initial sulphuric acid concentrations of $1.2 \times 10^7 \text{ molecules cm}^{-3}$ followed by sustained acid concentrations of greater than $6 \times 10^7 \text{ molecules cm}^{-3}$ resulting from high DMS concentrations of the order of 400 ppt. DMS concentrations of 100 ppt and high wind speed resulted in minor enhancement of detectable particles (<10%) suggesting that this concentration and ammonia and sulphuric acid may represent a threshold for production of detectable particle enhancement. Lower DMS concentrations of 20 ppt led to significant nucleation, but none of these were able to grow to detectable sizes. These results for the MBL support the concept of thermodynamically stable sulphate clusters, produced by ternary nucleation, providing the source of nuclei for MBL aerosol; however, this source can only be realised under extreme, or sustained sulphuric acid concentrations; an additional source of condensable material; or infrequent reduction of the preexisting aerosol condensation sink due to precipitation. Given a quasi-static background sulphate aerosol population, wind-generated sea-salt aerosol is more likely to control the production of new particles due to its contribution to the MBL aerosol condensation sink. Taking into account the uncertainties in the theoretical assumptions, it is plausible that the background MBL aerosol concentration could be maintained by a slow, almost undetectable production rate and not by noticeable nucleation events where large enhancements in detectable particle concentrations are observed. The former requires sustained DMS concentrations of the order of 100 ppt which seems unlikely. In the event, however, of significant removal of the preexisting aerosol due to precipitation, the MBL aerosol can be replenished through growth of new particle formed through ternary nucleation under moderate DMS concentrations.

Acknowledgments: This work was supported by the European Union under contracts ENV4-CT97-0526 (PARFORCE) and ENV4-CT98-0405 (BIOFOR).

References

- Allen, M.D., and O.G. Raabe, Slip correction measurements of spherical solid aerosol particles in an improved Millikan apparatus, *Aerosol Sci. Technol.* **4**, 269-286, 1985.
- Andreae, T.W., M.O. Andreae, and G. Schebeske, Biogenic sulfur emissions and aerosols over the tropical South Atlantic, 1. Dimethylsulfide in sea-water and in the atmospheric boundary layer, *J. Geophys. Res.* **99**, 22,819-22,829, 1994.
- Andreae, M.O., W. Elbert, and J. de Mora, Biogenic sulfur emissions and aerosols over the tropical South Atlantic. 3. Atmospheric dimethylsulfide, aerosols, and cloud condensation nuclei, *J. Geophys. Res.* **100**, 11,335-11,356, 1995.
- Atkinson, R., D.L. Baulch, R.A. Cox, Jr.R. F. Hampson, J.A. Kerr, M.J. Rossi, and J. Troe, Evaluated kinetic and photochemical data for atmospheric chemistry: Supplement V, IUPAC Subcommittee on Gas Kinetic Data Evaluation for Atmospheric Chemistry, *Atmos. Environ.* **30**, 1996.
- Ayers, G. P., R. W. Gillett, and J. L. Gras On the vapor pressure of sulfuric acid, *Geophys. Res. Lett.*, **7**, 433-436, 1980.
- Baker, M. B., and R.J. Charlson, Bistability of CCN concentrations and thermodynamics in the cloud-topped boundary layer, *Nature*, **353**, 834-835, 1990.
- Bandy, A.R., D.L. Scott, B.W. Blomquist, S.M. Chen, and D.C. Thornton, Low yields of SO_2 from dimethyl sulfide oxidation in the marine boundary layer, *Geophys. Res. Lett.*, **19**, 1125-1127, 1992.
- Bates, T.S., J.D. Cline, R.H. Gammon, and S.R. Kelly-Hansen, Regional and seasonal variations in the flux of oceanic dimethylsulfide to the atmosphere, *J. Geophys. Res.*, **92**, 2930-2938, 1987.
- Berresheim, H., J.W. Huey, R.P. Thorn, F.L. Eisele, D.J. Tanner, and A. Jefferson, Measurements of dimethyl sulfide, dimethyl sulfoxide, dimethyl sulfone, and aerosol ions at Palmer Station, Antarctica, *J. Geophys. Res.*, **103**, 1629-1637, 1998.
- Capaldo, K.P., P. Kasibhatla, and S. N. Pandis, Is aerosol production within the remote marine boundary layer sufficient to maintain observed concentrations? *J. Geophys. Res.*, **104**, 3483-3500, 1999.
- Clarke, A.D., et al., Particle nucleation in the tropical boundary layer and its coupling to marine sulfur sources, *Science*, **282**, 89-91, 1998.
- Covert, D.S., V. N. Kapustin, T.S. Bates, and P.K. Quinn, New particle formation in the marine boundary layer, *J. Geophys. Res.*, **97**, 20,581-20,589, 1992.
- Covert, D.S., V.N. Kapustin, P.K. Quinn, and T.S. Bates, Physical properties of marine boundary layer aerosol particles of the mid-Pacific in relation to sources and meteorological transport, *J. Geophys. Res.*, **101**, 6919-6930, 1996.
- Davison, B., C.D. O'Dowd, C.N. Hewitt, R.M. Harrison, M. Schwikowski, U. Baltensperger, and M.H. Smith, Dimethyl sulphide, methane sulphonic acid and physico-chemical aerosol properties of in Atlantic air from the UK to Halley Bay, *J. Geophys. Res.*, **101**, 22,855-22,867, 1996.
- Dinger, J.E., H.B. Howell, and T.A. Wojciechowski, On the source and composition of cloud nuclei in a subsident air mass over the North Atlantic, *J. Atmos. Sci.*, **27**, 971-979, 1970.
- Durkee, P., et al., The impact of ship produced aerosols on the microphysical characteristics of warm stratocumulus clouds: A test of Hypotheses 1.1a and 1.1b, *J. Atmos. Sci.*, **57**, 2554-2569, 2000.
- Easter, R.C., and L.K. Peters, Binary homogeneous nucleation: Temperature and relative humidity fluctuations, nonlinearity, and aspects of new particle production in the atmosphere. *J. Appl. Meteorol.*, **33**, 775-784, 1994.
- FORTTRAN-routine D02EJF, The NAG Workstation Library Handbook 1. The Numerical Algorithms Group Ltd., Oxford, England, 1990.
- Fuchs, N. A., *The Mechanics of Aerosols*, Pergamon, Tarrytown, N.Y., 1964.
- Fuchs, N.A. and A.G. Sutugin, *Highly Dispersed Aerosols*. Butterworth-Heinemann Woburn, Mass., 1970.
- Haataja, J. and T. Vesala, (eds.), SMEAR II station for measuring forest ecosystem-atmosphere relations, *Publ. 17*, 100 pp, Department of Forest Ecology, University of Helsinki, 1997.
- Hegg, D.A., Heterogeneous production of CCN in marine atmospheres, *Geophys. Res. Lett.*, **17**, 2165-2168, 1990.
- Hegg, D.A., Particle production in clouds, *Geophys. Res. Lett.*, **18**, 995-998, 1991.
- Hegg, D.A., L.F. Radke and P.V. Hobbs, Particle production associated with marine clouds, *J. Geophys. Res.*, **95**, 13,917-13,926, 1990.
- Hoppel, W.A., G.M. Frick, J.W. Fitzgerald, R.E. Larson, and E.J. Mack, Atmospheric aerosol size distributions and optical properties in the marine boundary layer over the Atlantic ocean, *NRL Rep. 9188*, Natl. Res. Lab., Washington D.C. 1989.
- Hoppel, W.A., G.M. Frick, J.W. Fitzgerald, and R.E. Larson, Marine boundary layer measurements of new particle formation and the effects nonprecipitating clouds have on the aerosol size distribution, *J. Geophys. Res.*, **99**, 14,443-14,459, 1994.
- Houghton, J.T., L.G. Meria Filho, B.A. Callendar, N. Harris, A. Katzenberg, and K. Maskell (Eds.) *Climate Changes: The Science of Climate Change*, Cambridge Univ. Press, New York, 1995.
- Jaeger-Voirol, A., A.P. Mirabel, and H. Reiss, Hydrates in supersaturated binary sulphuric acid-water vapor: A reexamination., *J. Chem. Phys.*, **87**, 4849-4852, 1987.
- Jefferson, A., D.J. Tanner, F.L. Eisele, and H. Berresheim, Sources and sinks of H_2SO_4 in the remote Antarctic marine boundary layer, *J. Geophys. Res.*, **103**, 1639-1647, 1998.
- Katoshevski, D., A. Nenes, and J.H. Seinfeld, A study of processes that govern the maintenance of aerosols in the marine boundary layer, *J. Aerosol. Sci.*, **30**, 503-532, 1999.
- Kerminen V.-M., Pirjola L., Boy M., Eskola A., Teinilä K., Laakso L., Asmi A., Hienola J., Lauri A., Vainio V., Lehtinen K. and Kulmala M. Interaction between SO_2 and submicron atmospheric particles. *Atmos. Res.* **54**, 41-57, 2000.
- Korhonen, P., M. Kulmala, A. Laaksonen, Y. Viisanen, R. McGraw, and J.H. Seinfeld., Ternary nucleation of H_2SO_4 , NH_3 , and H_2O in the atmosphere, *J. Geophys. Res.*, **104**, 26,349-26,353, 1999.
- Kreidenweis, S.M., and J.H. Seinfeld, Nucleation of sulfuric acid-water and methanesulfonic acid water solution particles, Implications for the

- atmospheric chemistry of organosulfur species, *Atmos. Environ.*, **23**, 2053-2057, 1988.
- Kulmala, M., *Simulating the Formation of Acid Aerosols. Acidification in Finland*, edited by P. Kauppi, P. Anttila, and K. Kenttämies, pp. 95-110, Springer-Verlag, New York, 1990.
- Kulmala, M., Ü. Rannik, E.L., Zapadinsky, and C.F. Clement., The effect of saturation fluctuations on droplet growth. *J. Aerosol Sci.*, **28**, 1395-1409, 1997.
- Kulmala, M., A. Laaksonen, and L. Pirjola, Parameterizations for sulphuric acid/water nucleation rates. *J. Geophys. Res.*, **103**, 8301-8307, 1998.
- Kulmala, M., L. Pirjola, and J.M. Mäkelä, Stable sulphate clusters as a source of new atmospheric particles. *Nature*, **404**, 66-69, 2000.
- Lin, X. and W.L. Chameides, CCN formation from DMS oxidation without SO₂ acting as an intermediate. *Geophys. Res. Lett.*, **20**, 579-582, 1993.
- Lin, X., W.L. Chameides, C.S. Kiang, A.W. Stelson, and H. Berresheim, A model study of the formation of clouds condensation nuclei in remote marine areas. *J. Geophys. Res.*, **97**, 18,161-18,171, 1992.
- Nilsson, E.D. and M. Kulmala, The potential for atmospheric mixing processes to enhance the binary nucleation rate. *J. Geophys. Res.*, **103**, 1381-1389, 1998.
- Nilsson, E.D., L. Pirjola, and M. Kulmala, The effect of atmospheric waves on aerosol nucleation and size distribution. *J. Geophys. Res.*, **105**, 19917-19926, 2000.
- O'Dowd, C.D. and M.H. Smith. Physico-chemical properties of aerosol over the Northeast Atlantic: Evidence for wind speed related sub-micron sea-salt aerosol production. *J. Geophys. Res.*, **98**, 1137-1149 1993.
- O'Dowd, C.D., M.H. Smith and S.G. Jennings. Submicron aerosol, radon and soot carbon characteristics over the Northeast Atlantic. *J. Geophys. Res.*, **98**, 1123-1136, 1993.
- O'Dowd, C.D., J.A. Lowe and M.H. Smith, Marine aerosol, sea-salt, and the marine sulphur cycle: A short review. *Atmos. Environ.* **31**, 73-80, 1997a.
- O'Dowd, C.D., B. Davison, J.A. Lowe, M.H. Smith, R.M. Harrison, and C.N. Hewitt, Biogenic sulphur emissions and inferred sulphate CCN concentrations in and around Antarctica. *J. Geophys. Res.*, **102**, 12,839-12,854, 1997b.
- O'Dowd, C.D., M. Geever, M.K. Hill, S.G. Jennings, and M.H. Smith, New particle formation: Spatial scales and nucleation rates in the coastal environment. *Geophys. Res. Letts*, **25**, 1661-1664, 1998.
- O'Dowd, C.D., et al., On the photochemical production of new particles in the coastal boundary layer. *Geophys. Res. Lett.*, **26**, 1707-1710, 1999a.
- O'Dowd, C.D., J. A. Lowe, M.H. Smith and A.D. Kaye, The relative importance of sea-salt and nss-sulphate aerosol to the marine CCN population: An improved multi-component aerosol-droplet parameterisation. *Q. J. Roy. Met. Soc.*, **125**, 1295-1313, 1999b.
- O'Dowd, C.D., J.A. Lowe, and M.H. Smith, Coupling sea-salt and sulphate interactions and its impact on predicting cloud droplet concentrations. *Geophys. Res. Lett.* **26**, 1311-1314, 1999c.
- O'Dowd, C.D., J.A. Lowe, N. Clegg, S.L. Clegg and M.H. Smith, Modelling heterogeneous sulphate production in maritime stratiform clouds. *J. Geophys. Res.* **105**, 7143-7160, 2000.
- Osborne, S. R., D. W. Johnson, R. Wood, B. J. Bandy, M. O. Andreae, C. D. O'Dowd, P. Glantz, K. Noone, C. Gerbig, Jochen Rudolph, T.S. Bates, and P. Quinn, Evolution of the aerosol, cloud and boundary layer dynamic and thermodynamic characteristics during the 2nd Lagrangian experiment of ACE-2, *Tellus*. **52B**, 375-400, 2000.
- Pandis, S.N., L.M. Russell, and J.H. Seinfeld, The relationship between DMS flux and CCN concentration in remote marine regions. *J. Geophys. Res.*, **99**, 16,945-16,957, 1994.
- Pandis, S.N., L.M. Russell and J.H. Seinfeld, Reply to Comment on "The relationship between DMS flux and CCN concentration in remote marine regions" by S.N. Pandis, L.M. Russell, and J.H. Seinfeld. *J. Geophys. Res.*, **100**, 14,357-14,358, 1995.
- Pirjola, L., Effects of the increased UV radiation and biogenic VOC emissions on ultrafine sulphate aerosol formation. *J. Aerosol Sci.*, **30**, 355-367, 1999.
- Pirjola, L., and M. Kulmala, Modelling the formation of H₂SO₄-H₂O particles in rural, urban and marine conditions. *Atmos. Res.*, **46**, 321-347, 1998.
- Pirjola, L., M. Kulmala, M. Wilck, A. Bischoff, F. Stratmann, and E. Otto, Formation of sulphuric acid aerosols and cloud condensation nuclei: an expression for significant nucleation and mode comparison. *J. Aerosol. Sci.*, **30**, 1079-1094, 1999.
- Preining, O., P.E. Wagner, F.G. Pohl, and W. Szymanski, *Heterogeneous Nucleation and Droplet Growth*, Inst. of Exp. Phys., University of Vienna, Vienna, Austria., 1981.
- Pruppacher, H.R., and J.D. Klett, *Microphysics of Clouds and Precipitation*, D. Reidel, Norwell, Mass., 1978.
- Radke, L.F., and P.V. Hobbs, Humidity and particle fields around some small cumulus clouds. *J. Atmos. Sci.*, **48**, 1190-1193, 1991.
- Raes, F., Entrainment of free tropospheric aerosols as a regulating mechanism for cloud condensation nuclei in the remote marine boundary layer. *J. Geophys. Res.*, **100**, 2893-2903, 1995.
- Raes, F., and A. Janssens, Ion-induced aerosol formation in a H₂O-H₂SO₄ system, II. Numerical calculations and conclusions. *J. Aerosol Sci.*, **17**, 715-722, 1986.
- Raes, F. and R. Van Dingenen, Simulations of condensation and cloud condensation nuclei from biogenic SO₂ in the remote marine boundary layer. *J. Geophys. Res.*, **97**, 12,901-12,912, 1992.
- Raes, F., and R. Van Dingenen, Comment on "The relationship between DMS flux and CCN concentration in remote marine regions" by S.N. Pandis, L.M. Russell, and J.H. Seinfeld. *J. Geophys. Res.*, **100**, 14,355-14,356, 1995.
- Ravishankara, A.R., Heterogeneous and multiphase chemistry in the troposphere. *Science*, **276**, 1058-1065, 1997.
- Reid, R.C., J.M. Prausnitz, and B.E. Poling, *The Properties of Gases and Liquids*, 4th ed., pp. 741, McGraw-Hill, New York, 1987.
- Russell, L.M., S.N. Pandis, and J.H. Seinfeld, Aerosol production and growth in the marine boundary layer. *J. Geophys. Res.*, **9**, 20,989-21,003, 1994.
- Sabelfeld, K.K., *Monte Carlo Methods in Boundary Value Problems*, *Comput. Phys. Ser.* edited by C.A.J. Fletcher et al., Springer-Verlag, New York, 1991.
- Sabinina, L. and L. Terpugow, Die Oberflächenspannung des Systems Schwefelsäure - Wasser. *Z. Phys. Chem. A* **173**, 237-241, 1935.
- Saltelli, A. and J. Hjort, Uncertainty and sensitivity analyses of OH-initiated dimethyl sulphide [DMS] oxidation kinetics. *J. Atmos. Chem.* **21**, 187-221, 1995.
- Schack, C.J. Jr., S.E. Pratsinis, and S.K. Friedlander, A general correlation for deposition of suspended particles from turbulent gases to completely rough surfaces. *Atmos. Environ.* **19**, 953-960, 1985.
- Sievering, H., J. Boatman, J. Galloway, W. Keane, Y. Kim, M. Luria, and J. Ray, Removal of sulphur from the marine boundary layer by ozone oxidation in sea-salt aerosols. *Nature*, **360**, 571-573, 1992.
- Sievering, H., E. Gorman, T. Ley, A. Pzenny, M., Springer-Young, J. Boatman, Y. Kim, C. Nagamoto, and D. Wellman, Ozone oxidation of sulfur in sea-salt aerosol particles during the Azores Marine Aerosol and Gas Exchange experiment. *J. Geophys. Res.*, **100**, 23075-23081, 1995.
- Simpson, D., Long-period modelling of photochemical oxidants in Europe: Model calculation for July 1985. *Atmos. Environ. Part A*, **26**, 1609-1634, 1992.
- Slingo, A., Sensitivity of the Earth's radiation budget to changes in low clouds. *Nature*, **343**, 49-51, 1990.
- Taleb, D.-E., J.-L. Ponche, and P. Mirabel, Vapor pressures in the ternary system water-nitric acid-sulfuric acid at low temperature: A reexamination. *J. Geophys. Res.*, **101**, 25967-25977, 1996.
- Viisanen, Y., M. Kulmala, and A. Laaksonen, Experiments on gas-liquid nucleation of sulfuric acid and water. *J. Chem. Phys.*, **107**, 920-926, 1997.
- Weber, R.J., et al., A study of new particle formation and growth involving biogenic trace gas species measured during ACE-1. *J. Geophys. Res.*, **103**, 16385-16396, 1998.
- Weber, R.J., et al., New particle formation in the remote troposphere: A comparison of observations at various sites. *Geophys. Res. Lett.*, **26**, 307-310, 1999.
- Wilemski, G., Composition of the critical nucleus in multicomponent vapor nucleation. *J. Chem. Phys.*, **80**, 1370-1372, 1984.
- Yin, F., D. Grosjean, and J.H. Seinfeld, Photooxidation of dimethyl sulphide, I, mechanism development. *J. Atmos. Chem.* **11**, 309-364, 1990.

I.M. Brooks, Scripps Institution of Oceanography, 9500 Gilman Drive, La Jolla, CA 92093-0230.

M. Kulmala, C.D. O'Dowd, (corresponding author) and L. Pirjola, Department of Physics, PO Box 9, FIN00014, University of Helsinki, Helsinki. (cdodowd@eircom.net)

(Received March 2, 2000; revised May 17, 2000; accepted May 19, 2000.)